Sign Variation in the Magnetic Circular Dichroism Spectra of Free-Base Porphyrins Having a Single π-Acceptor Pyrrole Ring Substituent. Structure Implications[1]

Carl Djerassi,* Yucheng Lu,[2a] Ahmad Waleh,[2b] Arthur Y. L. Shu, Robert A. Goldbeck, Lisa A. Kehres, Christopher W. Crandell, Andrew G. H. Wee, Andreas Knierzinger, Richard Gaete-Holmes, Gilda H. Loew,*[2b] Peter S. Clezy,[2c] and Edward Bunnenberg

Contribution from the Department of Chemistry, Stanford University, Stanford, California 94305, the School of Chemistry, University of New South Wales, Kensington, Australia 2033, and the Molecular Theory Laboratory, Rockefeller University, Palo Alto, California 94304. *Received September 27, 1983*

Abstract: The results of the first coherent investigation of the absorption and magnetic circular dichroism spectra of a series of monosubstituted free-base porphyrins possessing vinyl, cyano, ethoxycarbonyl, acetyl, and formyl substituents are reported. Dipole strengths and B values are obtained by curve-fitting and moment analysis of the lowest energy Q_0^x, Q_1^x, Q_0^y, and Q_1^y transitions. These values for the Q_0^x and Q_0^y transitions along with dipole strength and magnetic molar ellipticity data for the Soret transitions are used to compare the responses of the porphyrin and benzene π systems to the electronic demands of the substituents. Marked differences are found, and these are related to steric interactions and N–H proton tautomerism which are the structural features distinguishing the two π systems. Absorption spectral changes are treated within the context of Gouterman's four-orbital model, and the occurrences of MCD band sign variation throughout the series are related to structural perturbations using Michl's perimeter model. Additional theoretical insight into, and the tracking of, the orbital energy shifts attending the interaction of conformational and tautomerism effects is gained from INDO/S calculations. Finally, since the structural effects are manifest only at relatively weak absorption and magnetic circular dichroism signal strengths, careful and explicit consideration is taken of the extent to which low-frequency vibrational bands within and near the Q_0^x envelopes may obscure the elicitation of structurally significant information.

Introduction

Substituent-induced sign variation is a well known and often studied phenomenon in the magnetic circular dichroism (MCD) spectroscopy of organic molecules, and examples of its occurrence span a wide range from simple saturated ketones[3] to a variety of complex multi-ring π-electron systems. It was first reported for substituted benzenes by Foss and McCarville[4] who observed that the sign of the MCD associated with the ^1L_b transition was related to whether the substituent was an ortho–para or meta directing group. Subsequently, the additional experimental and theoretical work of several groups[5–9] on simple substituted benzene derivatives has placed the sign variation phenomenon on a more secure theoretical basis. Sign variation owing to the presence of electron-withdrawing and electron-donating substituents at different positions of a number of other cyclic π-electron substrates such as naphthalene,[10] anthracene,[11] pyrene,[12] 1,6-methano[10]-annulene,[13] and pyridine[14] have also been reported. These and parallel studies on a variety of different aromatic systems have been instrumental in the development, elaboration, and testing of Michl's perimeter model[15] for relating the absolute signs of the MCD associated with the four lowest energy purely electronic transitions of cyclic π-electron systems to the relative magnitudes of the orbital energy differences between the two highest occupied (ΔHOMO) and the two lowest unoccupied (ΔLUMO) molecular orbitals. Reviews which emphasize the application of the model have appeared recently.[16]

MCD band sign inversion for molecules derived from the porphine chromophore was first observed for a series of metal-free chlorin derivatives.[17] The occurrence of sign inversion was attributed to the "chlorin perturbation", and it was noted that the presence of electron-withdrawing carbonyl substituents served merely to strongly modulate the intensity of the inverted MCD associated with the weak Q_0^x transition. Subsequently, a theoretical investigation of the MCD of reduced porphyrins was presented[18] and further experimental studies of chlorophyll a,[19] metal derivatives of chlorophyll a and b,[20] and bacteriochlorophyll derivatives[21] were made. More recently, an extensive experimental study coupled with a perturbed molecular orbital analysis of the MCD of a series of unsubstituted, alkyl-substituted, and tetraphenyl-substituted chlorins, bacteriochlorins, and isobacteriochlorins has been reported.[22]

(1) Part 65 in the Stanford Magnetic Circular Dichroism Series. For Part 64, see: Lu, Y.-C.; Shu, A. Y. L.; Knierzinger, A.; Clezy, P. S.; Bunnenberg, E.; Djerassi, C. *Tetrahedron Lett.* **1983**, 2433.

(2) (a) Beijing Institute of Chemical Reagents, Beijing, China. (b) Rockefeller University. (c) University of New South Wales.

(3) (a) Seamans, L.; Moscowitz, A.; Barth, G.; Bunnenberg, E.; Djerassi, C. *J. Am. Chem. Soc.* **1972**, *94*, 6464. (b) Seamans, L.; Moscowitz, A.; Linder, R. E.; Morrill, K.; Dixon, J. S.; Barth, G.; Bunnenberg, E.; Djerassi, C. *Ibid.* **1977**, *99*, 724. (c) Linder, R. E.; Morrill, K.; Dixon, J. S.; Barth, G.; Bunnenberg, E.; Djerassi, C.; Seamans, L.; Moscowitz, A. *Ibid.* **1977**, *99*, 727.

(4) Foss, J. G.; McCarville, M. E. *J. Am. Chem. Soc.* **1967**, *89*, 30.

(5) Shieh, D. J.; Lin, S. H.; Eyring, H. *J. Phys. Chem.* **1973**, *77*, 1031.

(6) Michl, J.; Michl, J. *J. Am. Chem. Soc.* **1974**, *96*, 7887.

(7) Kaito, A.; Tajiri, A.; Hatano, M. *J. Am. Chem. Soc.* **1976**, *98*, 384.

(8) Obbink, J. H.; Hezemans, A. M. F. *Theor. Chim. Acta* **1976**, *43*, 75.

(9) Kaito, A.; Hatano, M. *J. Am. Chem. Soc.* **1978**, *100*, 2034.

(10) Whipple, M. R.; Vasák, M.; Michl, J. *J. Am. Chem. Soc.* **1978**, *100*, 6844.

(11) Steiner, R. P.; Michl, J. *J. Am. Chem. Soc.* **1978**, *100*, 6861.

(12) Vasák, M.; Whipple, M. R.; Berg, A.; Michl, J. *J. Am. Chem. Soc.* **1978**, *100*, 6872.

(13) (a) Dewey, H. J.; Deger, H.; Frölich, W.; Dick, B.; Klingensmith, K. A.; Hohlneicher, G.; Vogel, E.; Michl, J. *J. Am. Chem. Soc.* **1980**, *102*, 6412. (b) Klingensmith, K. A.; Püttmann, W.; Vogel, E.; Michl, J. *Ibid.* **1983**, *105*, 3375.

(14) Wallace, S. L.; Castellan, A.; Muller, D.; Michl, J. *J. Am. Chem. Soc.* **1978**, *100*, 6828.

(15) (a) Michl, J. *J. Am. Chem. Soc.* **1978**, *100*, 6801. (b) Michl, J. *Ibid.* **1978**, *100*, 6812. (c) Michl, J. *Ibid.* **1978**, *100*, 6819.

(16) (a) Michl, J. *Pure Applied Chem.* **1980**, *52*, 1549. (b) Michl, J. *Tetrahedron Rept.*, in press.

(17) Briat, B.; Schooley, D. A.; Records, R.; Bunnenberg, E.; Djerassi, C. *J. Am. Chem. Soc.* **1967**, *89*, 6170.

(18) McHugh, A. J.; Gouterman, M.; Weiss, C. *Theor. Chim. Acta* **1972**, *24*, 346.

(19) Houssier, C.; Sauer, K. *J. Am. Chem. Soc.* **1970**, *92*, 779.

(20) Schreiner, A. F.; Gunter, J. D.; Hamm, D. J.; Jones, I. D.; White, R. C. *Inorg. Chim. Acta* **1978**, *26*, 151.

(21) (a) Sutherland, J. C.; Olson, J. M. *Photochem. Photobiol.* **1981**, *33*, 379. (b) Wright, K. A.; Boxer, S. G. *Biochemistry* **1981**, *20*, 7546.

(22) (a) Keegan, J. D.; Stolzenberg, A. M.; Lu, Y. C.; Linder, R. E.; Barth, G.; Moscowitz, A.; Bunnenberg, E.; Djerassi, C. *J. Am. Chem. Soc.* **1982**, *104*, 4305. (b) Keegan, J. D.; Stolzenberg, A. M.; Lu, Y. C.; Linder, R. E.; Barth, G.; Moscowitz, A.; Bunnenberg, E.; Djerassi, C. *Ibid.* **1982**, *104*, 4317.

0002-7863/84/1506-4241$01.50/0

Within the sphere of porphyrins proper, sign variation within the vibronic manifold of the Q_0 transition of D_{4h} porphyrins is well known,[23-25] and it may also occur within the electronic origin of perimeter symmetric centrally substituted porphyrins when the dipole strength is small.[23a,c,25,26] Within the purely electronic transitions of porphyrins of lower symmetry, sign inversion may arise in very special cases from symmetric substitution as is the case for tetrakis(pentafluorophenyl)porphyrin;[27] however, the usual requirement for MCD band sign inversion within an electronic transition of either free-base or centrally substituted porphyrins is the presence of an electron-withdrawing substituent, commonly a carbonyl group, at a peripheral position. The occurrence of such substituent-induced sign variation is well documented, but only for a rather limited range of substituents,[19,23a,28] and has been most often and concertedly examined by several groups for the formyl–vinyl substituted heme *a* of the biologically important terminal oxidase, cytochrome *c* oxidase.[29-32]

Notwithstanding the substantial number of examples cited above where MCD band sign variation is an important feature for the vibronic or electronic bands of porphyrins, there have been no systematic experimental or theoretical studies which examine sign variation among porphyrins with a range, either singly or in combination, of electron-donating or electron-accepting substituents at the pyrrole or meso positions and which include variation in the central substituents from free base to metallo derivatives. Equally important is the fact that there have been no systematic studies of the effects of peripheral substituents on the electronic absorption spectra of porphyrins since Platt[33] and Gouterman[34] examined the extensive but fragmentary Stern data collected during the 1930's.

In the ensuing years, progress in the techniques of porphyrin synthesis[35,36] coupled with substantial progress in the understanding of porphyrin electronic structure[37] and in the application of sophisticated computational models[38,39] to the solution of particular problems renders such a detailed study of the electronic structure and spectra of porphyrins not only feasible but imperative as well. Magnetic optical activity, particularly MCD, has a secure phenomenological basis largely due to the work of Stephens[40] and, because of the additional spectroscopic as well as utilitarian structural information evoked by it, provides further and specific impetus for a concerted study of porphyrin substituent effects.

In the present work we report on our investigation of a series of free-base porphyrins (Figure 1) which contain vinyl, cyano, ethoxycarbonyl, acetyl, and formyl groups—a set of substituents which will be of continuing interest to us in other series of singly and multiply substituted porphyrins both with and without central substituents. The occurrence of sign variation will be considered, here, primarily within the context of Gouterman's four-orbital model of porphyrin electronic states[37,41] and within the context of Michl's perimeter model.[15,16] The series of correspondingly substituted benzene derivatives will serve as a point of reference, and differences in the occurrence of sign variation in the benzene and in the porphyrin series will be used to mark the incursion of stereochemical and N–H proton tautomerism effects which distinguish structural effects in the two series. In addition, the results of INDO/S calculations of the orbital energy distributions of the four frontier molecular orbitals will be used to test the conclusions based on naive four-orbital considerations and will be of further particular value in modeling the mutual interaction between the electronic character of the individual substituents on the one hand and the tautomeric and conformational structural events on the other. Finally, fine structural information appears primarily for the very weak Q_0^x transition and is consequently accompanied by a background of vibronic effects. This event forces the specific examination of the extent to which structural information is obscured by vibronic interactions.

Experimental Section. Experimental and Data Analysis Procedures

Materials. The structures of the porphyrins studied are given in Figure 1 along with the numbers that will be used throughout the text to refer to them. It will also be convenient to designate the porphyrins in a way which refers to the substituents and to the pattern of the extra nonchromophoric substituents which are also present. The trivial names for compounds 1 and **1a**, octaethylporphyrin and coproporphyrin II tetramethyl ester, respectively, will be shortened to OEP and Copro II. The letter P will be used to designate those porphyrins, e.g., P-CH=CH_2 (**2**), in the common series (**2–4**, **6**, and **8**) having methyl propionic ester side chains in the 3, 13, and 17 positions. MP-CN designates the cyano porphyrin (**7**) wherein a methyl group replaces the propionic ester group in position 13. DP-2-$COCH_3$ (**5**) designates one of the monoacetyl porphyrins derived from deuteroporphyrin IX dimethyl ester. These abbreviations along with the compound numbers are indicated in Table I.

The porphyrins were obtained from several sources. OEP (1) was a generous gift from H. H. Inhoffen. Copro II (**1a**) was obtained as a by-product in a separate synthetic study.[42] The porphyrins P-CH=CH_2 (**2**), P-$CO_2C_2H_5$ (**3**), P-$COCH_3$ (**4**), and P-CHO (**8**) were synthesized in one of our laboratories as previously described.[43a] The synthesis of MP-CN (**7**) has also been reported.[43b] Additional quantities of compounds **2**, **4**, and **8** were also synthesized at Stanford during the course of this study.[44]

The acetyl porphyrin (**4**) unexpectedly exhibited bisignate MCD within the Q_0^x transition (Figure 3), and in order to confirm this observation deuteroporphyrin IX dimethyl ester was acetylated according to the procedure of Brockmann et al.[45] The isomers were separated by chromatography and identified as prescribed by Clezy and Diakiw.[46] The MCD spectra of both monoacetyl derivatives are nearly identical, and the absorption and MCD spectra of the isomer studied, DP-2-CO-

(23) (a) Barth, G.; Linder, R. E.; Bunnenberg, E.; Djerassi, C. *Ann. N.Y. Acad. Sci.* **1973**, *206*, 223. (b) Linder, R. E.; Barth, G.; Bunnenberg, E.; Djerassi, C.; Seamans, L.; Moscowitz, A. *J. Chem. Soc., Perkin Trans. 2* **1974**, 1712. (c) Barth, G.; Linder, R. E.; Waespe-Sarcevic, N.; Bunnenberg, E.; Djerassi, C.; Aronowitz, Y. J.; Gouterman, M. *Ibid.* **1977**, 337.
(24) Perrin, M. H.; Gouterman, M.; Perrin, C. L. *J. Chem. Phys.* **1969**, *50*, 4317.
(25) Kielman-van Luijt, E. C. M.; Dekkers, H. P. J. M.; Canters, G. W. *Mol. Phys.* **1976**, *32*, 899.
(26) (a) Barth, G.; Linder, R. E.; Bunnenberg, E.; Djerassi, C. *J. Chem. Soc., Perkin Trans. 2* **1974**, 696. (b) Keegan, J. D.; Bunnenberg, E.; Djerassi, C. *Spectrochim. Acta, Part A* **1984**, *40*, 287.
(27) Keegan, J. D.; Bunnenberg, E.; Djerassi, C. *Spectrosc. Lett.* **1983**, *16*, 275.
(28) Gabriel, M.; Grange, J.; Niedercorn, F.; Selve, C.; Castro, C. *Tetrahedron* **1981**, *37*, 1913.
(29) Callahan, P. M.; Babcock, G. T. *Biochemistry* **1983**, *22*, 452.
(30) Kaito, A.; Nozawa, T.; Yamamoto, T.; Hatano, M.; Orii, Y. *Chem. Phys. Lett.* **1977**, *52*, 154.
(31) Woodruff, W. H.; Kessler, R. J.; Ferris, N. S.; Dallinger, R. F.; Carter, K. R.; Anitalis, T. M.; Palmer, G. *Adv. Chem. Ser.* **1982**, **No. 201**, 625.
(32) Thomson, A. J.; Englington, D. G.; Hill, B. G.; Greenwood, C. *Biochem. J.* **1982**, *207*, 167.
(33) Platt, J. R. "Radiation Biology"; Hollaender, A., Ed.; McGraw-Hill: New York, 1956; Chapter 2.
(34) Gouterman, M. *J. Chem. Phys.* **1959**, *30*, 1139.
(35) "Porphyrins and Metalloporphyrins"; Smith, K. M., Ed.; Elsevier: New York, 1975.
(36) "The Porphyrins"; Dolphin, D., Ed.; Academic Press: New York, 1978; Vol. I and II.
(37) Gouterman, M. "The Porphyrins; Dolphin, D., Ed.; Academic Press: New York, 1978; Vol. III, Chapter 1.
(38) (a) Waleh, A.; Loew, G. H. *J. Am. Chem. Soc.* **1982**, *104*, 3513. (b) Waleh, A.; Loew, G. H. *Ibid.* **1982**, *104*, 2346. (c) Waleh, A.; Loew, G. H. *Ibid.* **1982**, *104*, 2352. (d) Loew, G. H. In "Iron Porphyrins", Part I; Lever, A. B. P., Gray, H. B., Ed.; Addison-Wesley: Reading, MA, 1982; Chapter 1. (e) Pudzianowski, A. T.; Loew, G. H.; Mico, B. A.; Branchflower, R. V.; Pohl, L. R. *J. Am. Chem. Soc.* **1983**, *105*, 3434.
(39) Petke, J. D.; Maggiora, G. M.; Shipman, L. L.; Christoffersen, R. E. *J. Mol. Spectrosc.* **1978**, *71*, 64.
(40) (a) Buckingham, A. D.; Stephens, P. J. *Annu. Rev. Phys. Chem.* **1966**, *17*, 399. (b) Stephens, P. J. *J. Chem. Phys.* **1970**, *52*, 3489. (c) Stephens, P. J. *Adv. Chem. Phys.* **1976**, *35*, 197.
(41) (a) Gouterman, M. *J. Mol. Spectrosc.* **1961**, *6*, 138. (b) Gouterman, M.; Wagnière, G. H.; Snyder, L. C. *Ibid.* **1963**, *11*, 108. (c) Weiss, C.; Kobayashi, H.; Gouterman, M. *Ibid.* **1965**, *16*, 415.
(42) Wee, A. G. H.; Shu, A. Y. L.; Bunnenberg, E.; Djerassi, C. *J. Org. Chem.*, in press.
(43) (a) Chaudhry, I. A.; Clezy, P. S.; Diakiw, V. *Aust. J. Chem.* **1977**, *30*, 879. (b) Clezy, P. S.; Liepa, A. J. *Ibid.* **1971**, *24*, 1027.
(44) Shu, A. Y. L., unreported work; Ph.D. dissertation to be submitted to Stanford University.
(45) Brockmann, H.; Bliesener, K.-M.; Inhoffen, H. H. *Justus Liebigs Ann. Chem.* **1968**, *718*, 148.
(46) Clezy, P. S.; Diakiw, V. *Aust. J. Chem.* **1975**, *28*, 1589.

CH_3 (**5**), are nearly coincident with those of P-$COCH_3$ (**4**) as shown in Figure 1 of our preliminary communication.[1]

The cyano porphyrin MP-CN (**7**) exhibited a very unusual absorption spectrum (Figure 4) wherein two bands are clearly evident in the region of the Q_0^x transition. Since **7** had been synthesized[43b] with the cyano group in place at the pyrrole stage, which could have resulted in the presence of a small quantity of a very difficulty separable contaminant, the corresponding cyano porphyrin in the common series (i.e., P-CN, **6**) was prepared from the acetyl porphyrin P-$COCH_3$ (**4**) synthesized independently at Stanford. In this procedure,[44] P-$COCH_3$ was reduced to the 1-hydroxyethyl derivative with $NaBH_4$,[47a] dehydrated to the vinyl porphyrin (**2**) by heating with benzoyl chloride in dimethylformamide,[47b] and converted to the formyl derivative (**8**) by treatment with osmium tetroxide followed by sodium periodate, both steps being carried out in pyridine.[47c] P-CHO was converted to the oxime with subsequent dehydration to the cyano porphyrin (**6**) according to the selenium dioxide technique described by Sosnovsky et al.[48] Porphyrin products at the formyl, oxime, and cyano stages were particularly easy to separate, thereby ensuring the purity of P-CN (**6**). Spectra for P-CN and MP-CN are compared in Figure 4 where it will be observed that the pair of absorption bands in the region of the Q_0^x transition initially observed for MP-CN are also present for P-CN as well. Each of the compounds gave a satisfactory elemental analysis, and their MS, ^1H NMR, and absorption spectra were consistent with the structural features contained in each porphyrin.

The purity of each porphyrin was monitored by analytical TLC on Merck silica gel 60 F254 precoated (0.2 mm) sheets using several solvent systems appropriate to the particular porphyrin. When necessary (e.g., for P-CH=CH_2, **2**), porphyrins were purified by preparative TLC on glass plates coated with Merck silica gel 60G, which *does not* contain zinc sulfide as a fluorescent indicator. Because of the doubling of the absorption bands in the region of the Q_0^x transitions of P-CN (**6**) and MP-CN (**7**) and because of the differences in their MCD spectra (Figure 4), special efforts were made to ensure that both were free from even small quantities of impurities. After much experimentation it was found that the free base was the most suitable form for HPLC and that the best results were obtained using a semipreparative Whatman Partisil M9 10/50 ODS-3 column with 40% ethyl acetate in hexane as the eluent at a flow rate of 2 mL/min. Detection was via monochromator selected light at 405 nm. In this way small amounts of impurities (~1–2%) could be separated from MP-CN (**7**) whereas P-CN (**6**) was found to be free of contaminants.

The monosubstituted benzene derivatives styrene, benzonitrile, benzoic acid, ethyl benzoate, acetophenone, and benzaldehyde were of the highest purity (98 and 99%+) available from Aldrich and were used without further purification.

Spectroscopic Measurements. MCD measurements were made with a JASCO J-40 circular dichrometer whose calibration for CD was checked daily using an aqueous solution of *d*-10-camphorsulfonic acid monohydrate (Eastman) ($[\theta]_{290nm}$ = 7775 deg cm^2 dmol^{-1}, ref 49). The instrument is equipped with a JASCO electromagnet which provides a field of 14.7 kG as determined from an aqueous solution of $CoSO_4 \cdot 7H_2O$ (ultrapure, Research Organic/Inorganic Chemicals) for which $[\theta]_M$ = 6.2×10^{-3} deg cm^2 dmol^{-1} G^{-1} at 510 nm was reported by McCaffery et al.[50] A small nonlinearity (less than 1 nm) in the wavelength calibration was detected using a solution of holmium oxide in perchloric acid.[51] The 2-nm automatic spectral slit width program was routinely used for the broad-banded spectra provided by free-base porphyrins. Absorption spectra were taken on a Cary 14M spectrophotometer. Photometric performance was checked with a standard solution of KNO_3 or with several standard screens. Aldrich spectrophotometric grade chloroform (stabilized with 0.75% ethanol) was used for measurements of the free-base porphyrins. Care must be taken, however, in the routine use of chloroform since one of its decomposition products, hydrogen chloride, is especially pernicious for MCD measurements in that quite small amounts of the porphyrin dication distort the MCD spectra of the free bases as strongly as do metal complexes. To guard against this event, the integrity of the chloroform was checked each day with a freshly prepared solution of OEP. The concentrations of the porphyrins were such (about 0.4×10^{-4} M) that the optical density of the solution did not exceed 1.2 in the wavelength range of the measurement. Short-path cells (1 mm) and/or dilutions were used for measurements in the Soret region. Dichloromethane was used for low-temperature measurements since low sample solubilities precluded the use of common glass-forming solvents such as diethyl ether–isopentane–ethanol or toluene–diethyl ether. Temperatures were measured using an iron–constantan thermocouple immersed in the solution contained in a low-temperature cell holder previously described.[52] A correction factor of 1.15 was determined and used for absorption and MCD measurements in dichloromethane at 199 K to allow for solvent contraction.

Spectral Analysis Procedures. The band-shape function used previously (e.g., ref 23a) and here in the curve-fitting routines utilizes a variable wing model developed by Fraser and Suzuki.[53] The advantage of this model is that the wings of the shape function can be varied independently of the half-width and peak height, thereby providing an extra degree of freedom. This feature is extensively used here (vide infra) as a means of estimating the importance of low-frequency vibrational and/or extra electronic components within the MCD and absorption associated with the Q_0^x transition. The function is used in conjunction with a nonlinear least-squares curve-fitting procedure based on the method of Marquart.[54]

A variety of flexible programs were used for fitting absorption and MCD spectra and for extracting dipole strengths and values for the *B* term. The program SPECFIT allows an absorption or MCD curve to be fit separately and was used most often to obtain the values of *D* and *B* entered in Table I. The program SPECDDP allows simultaneous fitting of an absorption curve and its first derivative. Examples of its use to obtain spectral deconvolution over bands I and II of OEP and P-CN are shown in Figures 10 and 12. The program SPECABD permits simultaneous fitting of an absorption and MCD curve. An example of its use over band I of the acetyl porphyrin P-$COCH_3$ (**4**) is shown in Figure 11.

In the protocol for extracting parameters from an absorption spectrum, band I is fitted for each compound with the most care. First, the fitting range is restricted so that a "tight leading edge fit" (TLE fit) is obtained for the principal or leading component of band I. The dipole strengths so obtained are entered in Table I enclosed in square brackets. Then the fitting range is extended to the absorption minimum between bands I and II; the damping of the fitting parameters is set to zero and the fitting program is allowed to proceed to convergence. This procedure, termed the "full band fit" (FB fit), while distorting the position and half-width of the fitted band shape, picks up most of the absorption intensity in band I. The values for the dipole strengths obtained in this manner are unenclosed in Table I. The differences in the values of the dipole strengths of band I obtained by the two procedures thereby provides a measure of the additional electronic and/or vibronic components. The implications of these two values will be discussed, especially in the section "Vibronic MCD effects". The corresponding values for the dipole strengths obtained in dichloromethane at 295 and 199 K are also entered in Table III without enclosures.

The dipole strengths listed for bands II–IV in Table I were obtained from FB fits which do not explicitly include small satellite vibrational features. Thus, for each porphyrin the absorption intensity which leads to the shoulder on the blue side of band IV (marked by an asterisk in Figure 2) was excluded from the fit as was the small vibronic feature occasionally clearly evident (marked by a dagger in Figure 2) between bands I and II. The latter feature is, however, explicitly considered in the multiband fits shown in Figures 10 and 12. Finally, there is some uncertainty (about 10%) in the dipole strengths extracted for bands II–IV since the wing parameter is not well determined for absorption bands which overlap strongly.

Band I was treated with equal care in the protocol for analyzing the MCD spectra of the substituted porphyrins. For those porphyrins for which the MCD associated with the Q_0^x transition is monosignate, *B* values were extracted by the TLE fit protocol described above for absorption band I and are again entered in Table I enclosed within square brackets. In particular instances, P-$COCH_3$ (**4**) and DP-2-$COCH_3$ (**5**), a unique two-band fit was possible (Figure 11) and these values are entered in Table I without enclosure. In general, however, the most appropriate means of measuring the total *B* value for a band is via the zeroth moment,[40c,55] and the values obtained for the separate components along with B_{tot} are given in Table I and in Table III enclosed in braces.

(47) (a) Clezy, P. S.; Fookes, C. J. R. *Aust. J. Chem.* **1980**, *33*, 545. (b) Clezy, P. S.; Fookes, C. J. R.; Sternhell, S. *Ibid.* **1978**, *31*, 639. (c) Clezy, P. S.; Fookes, C. J. R. *Ibid.* **1980**, *33*, 575.

(48) Sosnovsky, G.; Krough, J. A.; Umhoefer, S. G. *Synthesis* **1979**, 722.

(49) Kreuger, W.; Pschigoda, L. M. *Anal. Chem.* **1971**, *43*, 675.

(50) McCaffery, A. J.; Stephens, P. J.; Schatz, P. N. *Inorg. Chem.* **1967**, *6*, 1614.

(51) McNeirney, J.; Slavin, W. *Appl. Opt.* **1962**, *1*, 365.

(52) Barth, G.; Dawson, J. H.; Dolinger, P. M.; Linder, R. E.; Bunnenberg, E.; Djerassi, C. *Anal. Biochem.* **1975**, *65*, 100.

(53) Fraser, R. D. B.; Suzuki, E. In "Spectral Analysis: Methods and Techniques"; Blackburn, J. A., Ed.; Marcel Dekker: New York, 1970; Chapter 5.

(54) Marquart, D. W.; Bennett, R. G.; Burrell, E. J. *J. Mol. Spectrosc.* **1961**, *7*, 269.

(55) (a) Schatz, P. N.; McCaffery, A. J. *Q. Rev., Chem. Soc.* **1969**, *23*, 552. (b) Stephens, P. J.; Mowery, R. L.; Schatz, P. N. *J. Chem. Phys.* **1971**, *55*, 224.

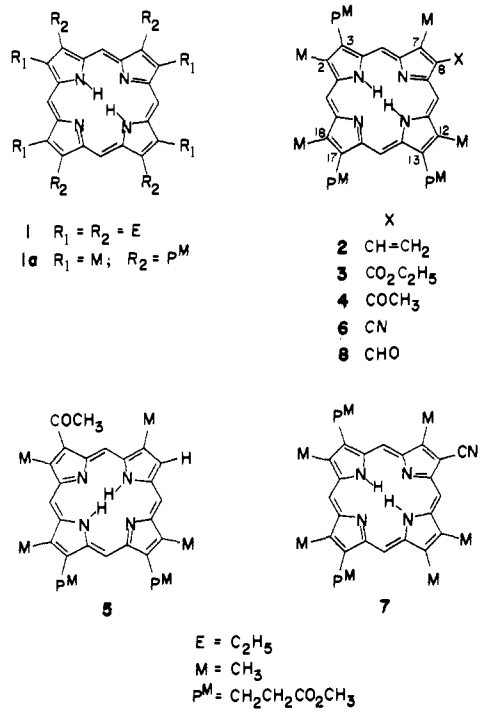

Figure 1. Structures of the metal-free monosubstituted porphyrins investigated.

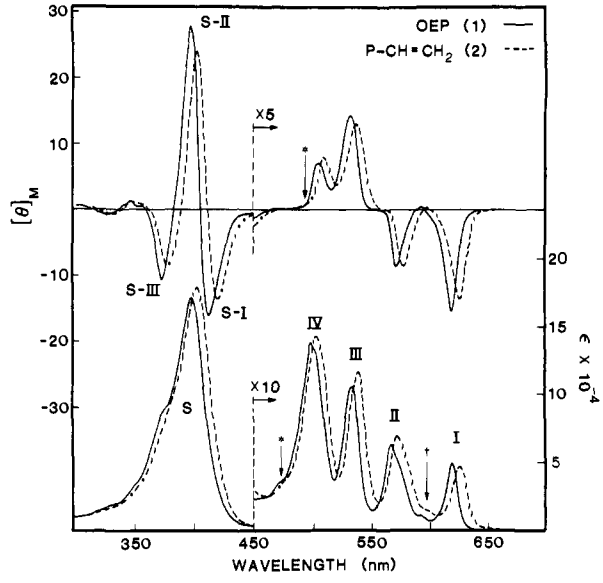

Figure 2. Absorption and magnetic circular dichroism spectra of octaethylporphyrin (1) (—) and monovinyl porphyrin 2 (---) in chloroform. The asterisk indicates portions of the absorption and MCD spectra which were excluded from the curve-fitting protocol for all porphyrins. The dagger indicates the small absorption band which was also excluded in the data analysis procedures.

B values were extracted without difficulty by curve-fitting for MCD bands II and IV; their values in Table I are unenclosed. This procedure has the advantage that MCD intensity on the blue edge of band IV (see asterisk in Figure 2) corresponding roughly to the excluded absorption intensity (vide supra) is also omitted from the *B* value obtained for band IV. *B* values for band III were extracted by curve-fitting where it was appropriate to do so (**1–5**, **8**) and otherwise (**6**, **7**) from the zeroth moment of the separate components.

Substituent effects in the Soret region are judged in MCD on the basis of peak values and in absorption on the basis of the sums of the dipole strengths of the main bands as indicated in Table I.

Results and Discussion

The structures of the compounds investigated in the present work are shown in Figure 1. In the common series P-CH=CH$_2$ (**2**), P-CO$_2$C$_2$H$_5$ (**3**), P-COCH$_3$ (**4**), P-CN (**6**), and P-CHO (**8**), the chromophoric substituents are contained in an otherwise identically substituted porphyrin. In addition to the porphyrins in the common series, further spectroscopic data have been obtained from the somewhat differently substituted porphyrins DP-2-COCH$_3$ (**5**) and MP-CN (**7**). Each of the chromophoric substituents chosen extends the π system of the substrate porphyrin ring and collectively they span a wide range from the weakly perturbing ±E vinyl group[56] to a strong π-acceptor (+E), the formyl group. Two porphyrins which contain only alkyl (octaethylporphyrin, OEP, **1**) or alkyl-like (coproporphyrin II tetramethyl ester, Copro II, **1a**) substituents are included as reference compounds against which to compare the effects of replacing an alkyl substituent with one of the chromophoric substituents.

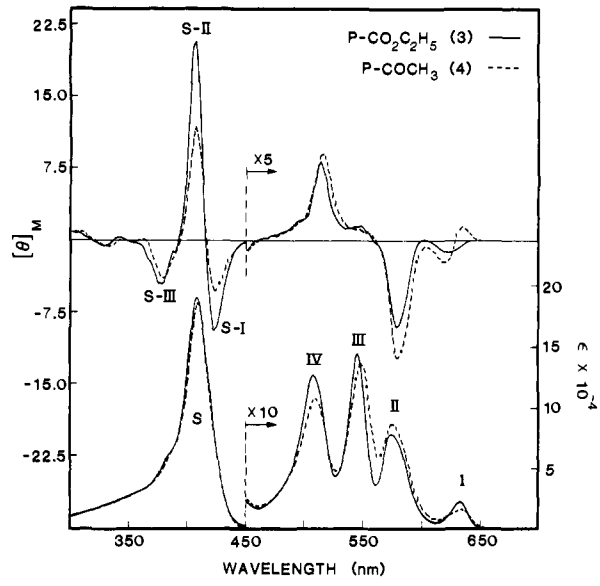

Figure 3. Absorption and magnetic circular dichroism spectra of monoethoxycarbonyl porphyrin 3 (—) and monoacetyl porphyrin 4 (---) in chloroform.

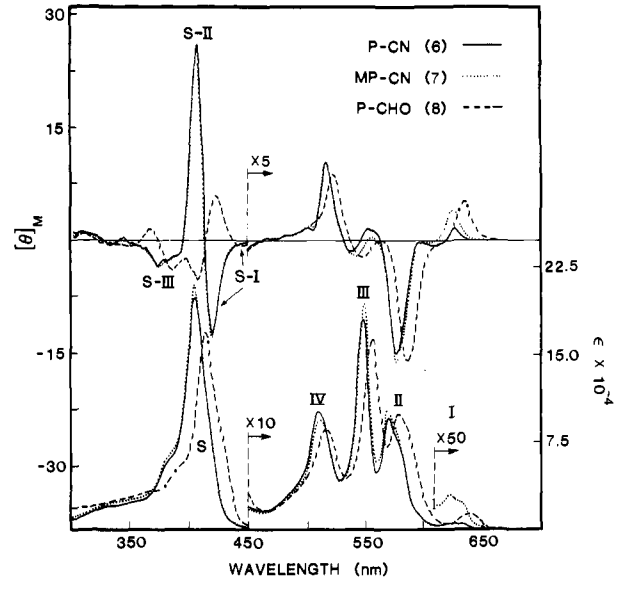

Figure 4. Absorption and magnetic circular dichroism spectra of monocyano porphyrin 6 (—), monocyano porphyrin 7 (. . .), and monoformyl porphyrin 8 (---) in chloroform.

(56) Dewar, M. J. S.; Dougherty, R. C. "The PMO Theory of Organic Chemistry"; Plenum Press: New York, 1975. This work contains a general treatment of some aspects of perturbation molecular orbital theory used here as well as definitions and categories of electromeric (E) and inductive (I) substituents and effects.

The absorption and MCD spectra of porphyrins **1–4** and **6–8** in chloroform solutions are shown in Figures 2–4. The spectra of DP-2-$COCH_3$ (**5**), which are essentially identical with those of **4**, were presented elsewhere.[1] The grouping is based primarily on similarities in their visible region MCD spectra and less on the π-acceptor character of the individual substituents. The bands labeled I and III correspond to the electronic Q_0^x and Q_0^y transitions, respectively, of free-base porphyrins whereas bands II and IV are the envelopes of their respective vibronic components.[37] The principal Soret region MCD peaks are labeled S-I, -II, and -III. Spectral data for all compounds are collected in Table I. Separate visible region spectral features which appear in either an absorption or an MCD spectrum and which appear to be components of a particular band are labeled as such (e.g., I_a, I_b). *B* values and dipole strengths were extracted by procedures outlined in the Experimental Section and are further annotated more specifically as necessary in the footnotes to Table I.

It should be noted that, with the definition of the Faraday parameters used here and in our previous papers, the sign of $[\theta]_M$ within a band is opposite to that of the *B* value of the band (see ref 57). For clarification, we will specifically note that "$[\theta]_M$ is + (or −). . ." or else will use the phrase "the MCD is + (or −). . ." for the same meaning. When it is necessary to refer to the *B* value of a band, we do so explicitly.

Spectra: General Aspects. Comparison of the absorption spectra shown in Figures 2–4 reveals that each of the substituted porphyrins exhibits, in addition to the strong Soret band at about 400 nm, the four visible bands which are generally characteristic of free-base porphyrins.[37] The visible spectra of OEP and P-CH=CH_2 (Figure 2) are referred to as etio spectra[58] because of the intensity ordering IV (Q_1^y) > III (Q_0^y) > II (Q_1^x) > I (Q_0^x). As the π-acceptor (+E) character of the substituent increases, the intensity pattern changes first (for P-$CO_2C_2H_5$, P-$COCH_3$, and DP-2-$COCH_3$) to the rhodo pattern[58] characterized by the intensity ordering of III > IV > II > I (Figure 3) and then to the ordering III > II > IV > I for the formyl porphyrin (Figure 4) which is, or borders on, the oxorhodo pattern observed more dramatically for porphyrins with +E substituents on opposed rings. The cyano porphyrins, **6** and **7** (Figure 4), exhibit the same intensity pattern as P-CHO, and their spectra are further marked by the appearance of two distinct components for band I. It was this occurrence that sparked the additional synthetic and purification work commented on in the experimental section. In addition to the redistribution in intensities of the visible bands owing to the presence of the substituents, it will be noted in Figures 2–4 that the Soret and visible bands also undergo a pronounced red shift throughout the series.

A similar broad survey of the MCD spectra of the substituted porphyrins shows that the Soret MCD of each porphyrin is comprised of three oppositely signed bands whose overall shape is that of a "W". The relative intensities of the component bands vary throughout the series although the central band is always the most intense. The intensity distribution among these bands and the fact that the symmetry of any porphyrin in the series is not higher than D_{2h} are consistent with the presence of at least three separate electronic transitions underlying the envelope of the Soret absorption band as is suggested by a number of calculations (e.g., ref 39). In the visible region, positive MCD (i.e., positive $[\theta]_M$) for band IV and negative MCD for band II are always observed regardless of the π-acceptor character of the substituent. On the other hand, the MCD varies much more dramatically for the electronic bands (bands I and III) throughout the series where the effects caused by the substituents range from hardly any for P-CH=CH_2 (**2**) (Figure 2), to a strong diminution in the intensities of the bands compared to OEP (P-$CO_2C_2H_5$, **3**, Figure 3), through cases (P-$COCH_3$, **4**, Figure 3; P-CN, **6**,

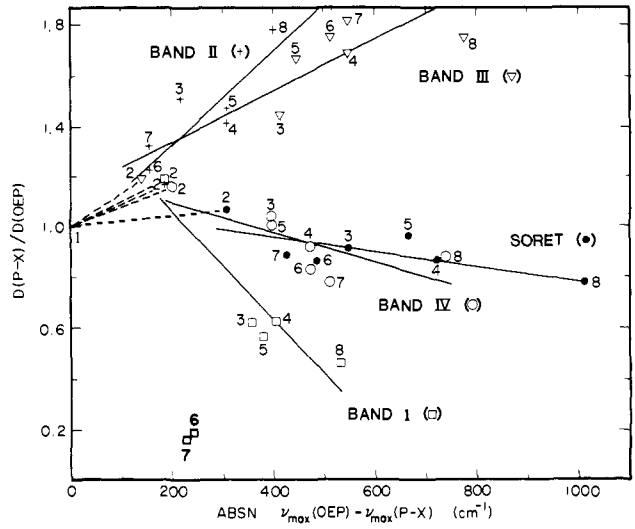

Figure 5. Comparison of the band shifts (cm^{-1}) and the relative changes in the dipole strengths of the Q_0^x (I), Q_1^x (II), Q_0^y (III), Q_1^y (IV), and Soret transitions of the substituted porphyrins with respect to octaethylporphyrin. The bold numbers designate data excluded from the linear least-squares fits (solid lines). The dashed lines emphasize the relation of the first data point (P-CH=CH_2, **2**) to octaethylporphyrin (**1**). The value of the $\Delta\nu$ for band I of the cyano porphyrins, **6** and **7**, is the average of the shifts for the two component bands (Ia and Ib).

Figure 4) where the MCD associated with one or both of bands I and III is bisignate, and finally to the case of P-CHO (**8**, Figure 4) for which the MCD of bands I and III is entirely inverted as compared to OEP (Figure 2). The positions of the MCD bands shift to the red throughout the series, as do the absorption bands; however, as is evident from the data in Table I, peak positions in an MCD spectrum rarely correspond exactly to those in the absorption spectrum.

Spectra–Specific Substituent Effect Correlations. The casual correlations of spectral band shifts, absorption band ratios, and the occurrence of MCD band sign inversions sketched briefly above provide only an approximate means of assessing the effect of a particular chromophoric substituent on porphyrin electronic spectra. Moreover, since our goal here is to use the data gathered to provide a more specific experimental estimate of how the substituents affect the energies of pertinent porphyrin molecular orbitals and to gauge the potential utility of MCD for deriving structurally useful information, we require a more quantitative analysis of the data.

Since the substituents evoke shifts in the energies of the porphyrin π–π^* transitions and changes in the intensities of the associated absorption and MCD bands, an appropriate method of quantitation of the effects of substituents is to consider energy shifts and intensity changes conjunctively and, further, to relate the changes to a reference porphyrin. OEP rather than Copro II (**1a**) is the more generally relevant reference porphyrin since throughout the much broader span of porphyrins which will be of continuing interest to us, the number of propionic ester groups present ranges from none to three. Comparison of the data in Table I shows that, as expected, their absorption and MCD spectra differ only in minor detail.

The data collected in Table I are analyzed in graphical form in Figures 5 and 6. Figure 5 contains plots of the ratio *D*(P-X)/*D*(OEP) for the corresponding absorption bands vs. the shifts in energies of these bands with respect to those of OEP. Correspondingly, changes in the visible region MCD spectra on progression through the series are correlated by plots of the ratios of the *B* values (Figure 6). To assist the reader in relating this plot to the spectra, we include in Figure 6 a specification of the *general direction* in which $[\theta]_M$ is changing for each band relative to OEP. It should also be noted in connection with Figure 6 that negative values for the *B*-value ratios indicate that the sign of the *B* term for the band is opposite to that for OEP. Finally, note that since the positions of the MCD bands are ambiguous in a

(57) The parameter definitions we have used conform to those of Stephens et al. (ref 60). Conversion to the "new" parameters of Stephens (ref. 40c) has been discussed in detail by Piepho, S. B.; Schatz, P. N. "Group Theory in Spectroscopy with Applications to Magnetic Circular Dichroism"; Wiley-Interscience: New York, 1983; pp 533–540.

(58) Reference 35, pp 20–23.

Table I. MCD and Absorption Spectral Data of Monosubstituted Free-Base Porphyrins[a]

compound[b]	spectrum	MCD[c]: $\lambda_{max}/[\theta]_M/10^{-4}B$ Soret and near-UV region	absorption:[d] $\lambda_{max}/10^{-3}\epsilon/D$ Q_I^y IV[e]	Q_0^y IIIb	Q_0^y IIIa	Q_I^x II[f]	Q_0^x Ib	Q_0^x Ia
OEP (1)	MCD	332 347 375 399 413	504	531		572	620	
		−0.9 1.3 −10.6 28.2 −16.0	1.4	2.8		−1.8	−3.1	
			−11.05	−26.27		11.0	{22.02}	
							[19.97]	
	ABSN	330 (s) 352 (s) 376 (s) 399	498	534		566	619	
		18.1 34.5 87.0 171.3	13.8	10.5		6.2	4.9	
		157.84	6.50	2.90		2.40	1.0	
							[0.84]	
Copro II (1a)	MCD	330 348 375 399 415	504	531		572	622	
		−1.2 1.3 −9.7 28.0 −16.4	1.4	2.5		−1.8	−2.8	
	ABSN	325 (s) 349 (s) 374 (s) 400	499	533		568	621	
		15.1 31.4 79.7 179.8	15.2	10.0		6.9	5.1	
P-CH=CH$_2$ (2)	MCD	332 349 379 404 422	508	535		577	626	
		−0.8 1.5 −8.6 24.2 −13.5	1.6	2.6		−1.7	−2.7	
			−16.02	−25.29		12.37	{21.61}	
							[19.43]	
	ABSN	332 (s) 354 (s) 380 (s) 404	503	538		572	626	
		16.5 32.0 90.3 178.8	14.2	11.6		7.0	4.6	
		167.2	7.56	3.46		2.80	1.19	
							[1.06]	
P-CO$_2$C$_2$H$_5$ (3)	MCD	332 378 408 424	514	547		579	623	
		−0.7 −4.4 20.7 −9.4	1.7	0.3		−1.8	−0.2	
			−17.16	−2.24		17.58	{2.76}	
							[2.77]	
	ABSN	330 (s) 350 (s) 380 (s) 408	508	546		573	633	
		19.4 26.3 52.0 189.2	12.7	14.4		7.8	2.3	
		143.88	6.74	4.20		3.63	0.62	
							[0.58]	
P-COCH$_3$ (4)	MCD	334 380 408 426	516	545 (s)		582	621 638	
		−0.7 −4.0 11.8 −5.4	1.8	0.2		−2.4	−0.5 0.3	
			−22.99	−1.61		25.0	{4.14} {−1.13}	
							5.46[g] −2.38[g]	
							B_{total} = {3.0}	
	ABSN	340 (s) 390 (s) 411	510	550		576	635	
		22.6 67.5 184.9	10.7	13.7		8.6	1.7[h]	
		135.29	6.0	4.91		3.39	0.62	
							[0.43]	
DP-2-COCH$_3$ (5)	MCD	328 343 379 408 425	514	555 (s)		581	622 636	
		−0.3 0.9 −4.5 12.3 −6.2	1.7	0.2		−2.4	−0.5 0.3	
			−20.77	−1.86		22.24	{3.50} {−1.63}	
							4.93[i] −3.21[i]	
							B_{total} = {1.87}	
	ABSN	335 (s) 390 (s) 410	508	547		576	6.34	
		23.8 76.8 200.7	11.3	13.5		8.3	1.6[j]	
		152.19	6.60	4.86		3.53	0.56	
							[0.46]	
P-CN (6)	MCD	360 (s) 376 393 (s) 406 421	516	539 555		577	611 628	
		−0.8 −3.5 −1.9 26.0 −12.3	2.1	−0.3 0.3		−3.0	−0.1 0.3	
			−15.63	{1.61} {−1.80}		25.13	{1.04} {−1.35}	
				B_{total} = {−0.19}			B_{total} = {−0.31}	
	ABSN	335 (s) 355 (s) 383 (s) 407	510	549		571	624 633 (s)	
		20.4 24.5 58.5 199.0	10.1	18.2		9.6	*k*, 0.63 0.57	
		135.46	5.41	5.08		2.94	0.14[l] 0.05[l]	
							D_{total} = 0.19	
MP-CN (7)	MCD	340 (s) 355 377 392 407 421	517	542 556		578	605 627	
		−0.6 −0.8 −3.6 −2.1 25.3 −12.7	2.0	−0.4 0.1		−3.2	~−0.06 0.8	
			−16.6	{2.93} {−0.27}		27.6	{0.22} {−5.2}	
				B_{total} = {2.66}			B_{total} = {−4.98}	
	ABSN	334 (s) 355 (s) 385 (s) 406	511	550		571	623 633 (s)	
		22.6 26.3 65.6 209.8	9.4	19.5		10.3	0.57 0.44	
		139.65	5.07	5.30		3.15	0.13[m] 0.03[m]	
							D_{total} = 0.16	
P-CHO (8)	MCD	344 368 387 408 423 447	522	547		587	636	
		−0.3 1.8 −4.0 −5.3 5.8 −0.7	1.7	−0.5		−3.2	1.0	
			−16.8	3.87		31.34	{−7.53}	
							[−8.1]	
	ABSN	345 (s) 371 (s) 394 416 427 (s)	517	557		579	640	
		27.1 33.7 55.7 169.8 93.1	8.8	16.4		10.0	1.4	
		121.27	5.72	5.08		4.28	0.46	
							[0.40]	

[a] Principal spectral features. The solvent is chloroform except for P-CO$_2$C$_2$H$_5$ (3) for which the solvent is dichloromethane. Dipole strengths and *B* values are tabulated only for clearly evident spectral features in the visible region. Selected additional results from curve-fitting are shown in Figures 10-12. [b] Structures are given in Figure 1. [c] Wavelength in nm; s = shoulder; molar magnetic ellipticity, $[\theta]_M$, in deg cm^2 dmol^{-1} G^{-1}; values for the *B* term of selected bands are in (Debye)^2 Bohr magneton/cm^{-1}; unenclosed values for the *B* term were

Table I (*Continued*)

obtained by curve-fitting (see Experimental Section). For band I a tight leading edge fitting protocol was used to obtain the values in square brackets. Values in braces were obtained from the zeroth moment. [d] Wavelength in nm; s = shoulder; molar extinction coefficient, ϵ, in 1000 cm^2 mol^{-1}; values for the dipole strength, D, of selected bands are in $(Debye)^2$; unenclosed values of D were obtained by curve-fitting. For band I, a tight leading-edge fit protocol was used to obtain the values enclosed in square brackets. The unenclosed values for band I were obtained by a full band (see Experimental Section) curve-fitting protocol and, unless otherwise noted, reflect the total intensity under the envelope of band I. They are thus comparable to values tabulated for bands II-IV. Soret dipole strengths are summed for the indicated bands. [e] The curve-fitting protocol excludes MCD and absorption vibronic intensity on the high energy edge of band IV for all compounds. The regions excluded are illustrated by the asterisk in Figure 2. [f] Dipole strengths do not include the small band between bands I and II. See, however, Figures 10 and 12 where they have been included in the fit. [g] Obtained by a simultaneous fitting of both the MCD and absorption spectra of 4; see Figure 11. [h] See Figure 13 for the data for the bands located by curve-fitting. [i] Obtained by a simultaneous fitting of both the MCD and absorption spectra of 5. See Figure 11 for the corresponding fit of 4. [j] Band can be located by curve-fitting in an analogous manner to that illustrated in Figure 11 for 4. [k] See Figure 12 for the extra band located by curve-fitting. [l] Dipole strengths obtained by the curve-fitting program SPECDDP (see Experimental Section). Values obtained for a three band fit are given in Figure 12. [m] Dipole strengths obtained by a direct two-band curve-fitting protocol.

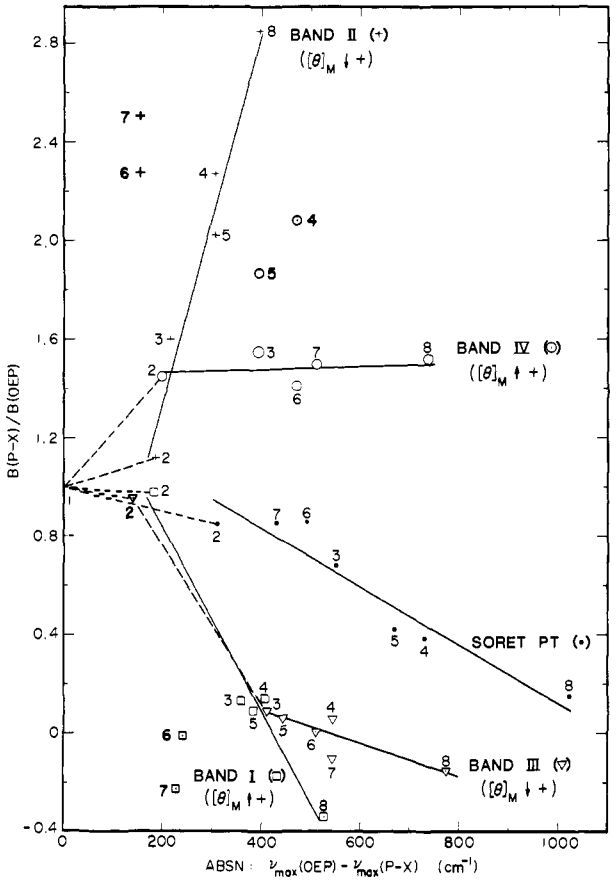

Figure 6. Comparison of the relative changes of the B values associated with the Q_0^x (I), Q_1^x (II), Q_0^y (III), and Q_1^y (IV) transitions of the substituted porphyrins with respect to those of octaethylporphyrin vs. the shift in energy (cm^{-1}) of the corresponding absorption band maxima. For the Soret MCD, the ratios of the peak-to-trough (PT) values of $[\theta]_M$ for MCD bands S-I and S-II $\{[\theta]_M(\text{S-II}) - [\theta]_M(\text{S-I})\}$ rather than B values are used. The occurrence of negative signs for the ratio of B values indicates MCD band sign inversion. Additional comments in the legend of Figure 5 are also relevant.

number of cases (e.g., band I for P-$COCH_3$ is bisignate, Figure 3), the ordinate axis for Figure 6 is again the shift in energy of the *absorption band maxima* with respect to OEP.

a. Soret Absorption and MCD Bands. Because of configuration interaction among singly excited porphyrin states, there is a relationship between the intensities of relevant Soret and visible transitions; however, since the Soret transitions are so strongly allowed and overlap, specific substituent effect correlations are tenuous. Notably, however, the dipole strengths for the porphyrins having +E substituents are smaller than those of OEP (Table I, Figure 5). It is also of interest that the increased splitting of the Soret band for P-CHO correlates with the fact that the separation in energies of its Q_0^x and Q_0^y transitions is the smallest in the present series, a correlation which was pointed out by Gouterman[34] in his preliminary presentation of the four-orbital model for substituted porphyrins.

There is no ambiguity in the Soret band shifts caused by the substituents since these range (Figure 5) from significant for the weakly perturbing vinyl group (about 300 cm^{-1}) to major for the more strongly perturbing formyl group (about 1000 cm^{-1}) with the cyano, ethoxycarbonyl, and acetyl shifts lying in that order between the two extremes.

Comparison of the spectra in Figures 2–4 shows that substituent-induced changes are much more pronounced in the Soret region MCD than they are in the absorption spectra. We have not attempted spectral deconvolution of the Soret MCD bands in order to obtain B values for the separate components but have, instead, in Figure 6 used ratios of the peak-to-trough values (PT) for MCD bands S-I and S-II of the substituted porphyrins to that for OEP as a measure of the effects of the substituents on the Soret MCD. This measure, while crude,[59] does indicate that the cyano group is about as effective as the vinyl group as far as perturbations in the Soret transitions are concerned and that the ethoxycarbonyl, acetyl, and formyl substituents again fall in a regular order.

A preliminary conclusion can be reached from the substituent-induced shifts in the positions of the Soret absorption band maxima *and* from the changes in the Soret PT values that the groups should be ordered CHO > $COCH_3$ > $CO_2C_2H_5$ > CN > $CH{=}CH_2$ with regard to their effects on the porphyrin π system. A somewhat different perspective of the effective ordering obtains from an analysis of the visible region absorption and MCD spectra of the substituted porphyrins given below.

b. Visible Region Absorption and MCD Bands. In contrast to the Soret states, electronic excitations into the Q states of free-base porphyrins, while formally allowed on symmetry grounds, are much weaker. A consequence of this is that the intensities of the visible transitions are much more sensitive to substituent effects than are those of the Soret transitions. This sensitivity has led, as previously noted, to the practical application of the etio, rhodo, and oxorhodo classifications of the relative intensities of bands I–IV as a first-order means of establishing porphyrin structures. In MCD, the sensitivity of the visible transitions to substituent effects leads to the possibility of sign variation, and the occurrence, or lack thereof, of this event carries with it the potential of an even more useful way of assessing substituent interactions with the porphyrin substrate.

(i) Absorption Band Energy Shifts. The visible transitions shift to lower energies; however, the shifts are markedly less in each case (Figure 5) as compared to the Soret band shift. It is also evident that, except for P-$CH{=}CH_2$ (**2**), the Q_0^y and Q_1^y bands (bands III and IV) shift equally and at a greater rate than do those of the transitions into the Q^x state (bands I and II). The ordering of the substituent-induced shifts for bands III and IV is CHO > $COCH_3$ ≈ CN > $CO_2C_2H_5$ > $CH{=}CH_2$. In contrast, in the Q^x transitions, with the exception of P-$CH{=}CH_2$, the vibronic band (band II) shifts less than does the electronic band (band I), and

(59) The PT value also measures, in part, the separation of the individual transitions within the Soret envelope. This is significant for P-CHO but less so for P-$CO_2C_2H_5$ and P-$COCH_3$ for which marked changes in the PT ratio occur without marked changes in the Soret half-width.

the ordering of the energy shifts is again the same as for the Soret band.

(ii) Absorption Intensity Changes. In the series following P-CH=CH_2 there is a marked decrease in the dipole strength of band I (Figure 5), with the ethoxycarbonyl and acetyl substituents (compounds **3**–**5**) having about the same effect and with the formyl group having only a somewhat greater effect (about 10%). Band I of the cyano porphyrins is quite unusual in several respects: it is composite in its band shape (Figure 4)—a unique occurrence we believe among published porphyrin spectra; the total dipole strength within the envelope is about 80% less than that within band I of OEP and is also much less than that of P-CHO (**8**); and the energy shifts of either of the components are not commensurate with the band intensity. As absorption intensity is lost in the Q_0^x transition owing to the effects of the substituents, intensity is gained in the next higher energy electronic transition Q_0^y (band III). The ordering is particularly clear for the carbonyl substituents (CHO > $COCH_3$ > $CO_2C_2H_5$).

As expected for the vibronic Q_1^x and Q_1^y absorption bands, it can be observed in the spectra given in Figures 2–4 but more clearly in the ratio plots of Figure 5 that as intensity is gained in the Q_0^y transition (band III) there is a decrease in the intensity of the associated vibronic band (band IV), and as the dipole strength of the Q_0^x transition (band I) decreases the amount of vibronically borrowed intensity increases (band II). Another view of this relationship to be gained from the data for the entire series in Table I is that the total dipole strength for transitions into the Q^y state $[D(Q_0^y + Q_1^y)]$ is nearly constant at an average value of 10.67 ± 0.27 D^2 while that for the Q^x state is 3.87 ± 0.88 D^2, this notwithstanding the wide range in the ratio $D(Q_0^y)/D(Q_0^x)$ from about 3 for OEP to about 30 for the cyano porphyrins.

(iii) MCD of Bands I–IV. Before commenting on the way in which the substituents affect the visible region MCD bands, we note two important aspects of MCD bands. First, it is pertinent to point out that intensity changes in *B*-term MCD bands do not necessarily parallel changes in the intensities of the corresponding absorption bands. This asynchronous behavior arises out of the differences in the quantum mechanical expression for the *B* term[40a] as compared to that for the dipole strength of a transition, $a \rightarrow j$:

$$B(a\rightarrow j) = Im\left\{\sum_{k\neq a}\frac{\langle k|\mu|a\rangle\cdot\langle a|\mathbf{m}|j\rangle \times \langle j|\mathbf{m}|k\rangle}{E_k - E_a} + \sum_{k\neq j}\frac{\langle j|\mu|k\rangle\cdot\langle a|\mathbf{m}|j\rangle \times \langle k|\mathbf{m}|a\rangle}{E_k - E_j}\right\}$$

$$D(a\rightarrow j) = |\langle a|\mathbf{m}|j\rangle|^2$$

where μ and $\mathbf{m}$ denote the magnetic and electric moment operators, respectively, and E_a, E_j, and E_k are the energies of the states *a*, *j*, and *k*, respectively. Thus, because of the scalar triple product form of the expression for the *B* term, if only two excited states *j* and *k* are coupled by the magnetic field and if the directions of the electric transition moments are not parallel, then the *B* terms of the two transitions $a \rightarrow j$ and $a \rightarrow k$ will be equal in magnitude but of opposite sign regardless of the disparity in the magnitudes of the dipole strengths of the two transitions.

Second, while sign variation may occur for the Q_0^x and Q_0^y transitions, the signs of the vibronic Q_1^x and Q_1^y MCD bands are invariant. A general explanation which has been offered[18,24,60,61] for the "cosignature" of the vibronic and electronic low-energy MCD bands of D_{2h} free-base porphyrins is that the reduction in symmetry from D_{4h} merely lifts the degeneracies of the vibronic and electronic Q states of the parent porphyrin. The electronic MCD bands in the D_{2h} porphyrin maintain their original D_{4h} sign pattern and the MCD of the vibronic transitions, made allowed in absorption by vibronic intensity borrowing from the Soret states due to the effects of both symmetric and nontotally symmetric vibrations, maintain their signs and become intermingled within the Q_1^x and Q_1^y envelopes. The overall signs and the contours[62] of the Q_1^x and Q_1^y MCD bands then reflect the complexities of the intermixing of the vibronic and electronic levels of the Q state among themselves and with the higher energy Soret states. In this context, the prevalence of the −+ sign pattern of the Q_1^x and Q_1^y MCD bands in the substituted porphyrins despite the occurrence of sign inversion in the electronic bands indicates that the cyclic polyene, free-base, perturbation[41a] is the largest perturbation present and that the substituents can be regarded as having a secondary effect.

Comparison of the spectra in Figures 2–4 and the data in Table I show that $[\theta]_M$ for band II becomes less positive through the series. This trend for $[\theta]_M$ corresponds to more positive values of $B(Q_1^x)$, and in the ratio of *B*-values plot given in Figure 6 there is relatively little scatter in the data points except for those of the cyano porphyrins (**6** and **7**) whose *B*-value ratios appear to be inordinately large. It will be recalled that the dipole strength of band II also increased throughout the series (Figure 5). Thus, in this instance absorption and MCD intensity both increase in magnitude and, in fact, excluding **6** and **7**, the ratio $B(Q_1^x)/D(Q_1^x)$ is relatively constant at 5.8×10^{-4} β_e/cm^{-1} with the variance ($\pm 1.56 \times 10^{-4}$ β_e/cm^{-1}) being attributable to curve-fitting uncertainties for the absorption bands and to differences in the details of the ways in which vibrations of different symmetry are revealed in the MCD as compared to the absorption spectrum.

Notwithstanding their vibronic origin, the MCD of bands II and IV is generally governed by the scalar triple product form of the expression (modified for vibronic wave functions) given for the *B* term above. Thus, MCD throughout bands II and IV will generally be of opposite sign although the contours may differ even if only intramanifold coupling is involved. Furthermore, except for complications of additional coupling, especially of the Q_1^y vibronic states with the nearby Soret states,[63] as $B(Q_1^x)$ becomes more positive $B(Q_1^y)$ should become more negative. This appears to be generally the case as the data points for P-CH=CH_2 (**2**), P-$COCH_3$ (**4**), and DP-2-$COCH_3$ (**5**) in Figure 6 indicate. For the other compounds in the series the *B*-value ratio for band IV is rather constant—an event which is due to the difficulty in accounting for the MCD intensity in band IV by curve-fitting and which reflects the fact that the MCD of band III becomes increasingly inverted in sign in the series P-$CO_2C_2H_5$ (**3**), P-CN (**6**), MP-CN (**7**), and P-CHO (**8**) (Figures 3 and 4).

The MCD associated with the Q_0^y transition should have an inverse sign relationship to that of the Q_0^x transition for the reasons already discussed. That this is the case is evident from the spectra given in Figures 2–4. However, it is difficult to accurately account for the MCD intensity in this band owing in large part to the overlap of the generally weaker band III with the stronger band IV. This is responsible for the shallow drop of the least-squares line for band III as compared with that for band I in Figure 6. Again note that the *B* values of band III are quite small but that the dipole strengths are large.

In contrast to the situation for the Q_0^y transition, both the MCD and absorption bands associated with the Q_0^x transition are well isolated from overlap by nearby strong vibrational bands. The MCD associated with the Q_0^x transition undergoes some dramatic changes (Figures 2–4) throughout the series, and it will be necessary here and in following sections to consider these in some detail both in terms of the *B* values for the MCD within the transition and in terms of the actual band shapes. $[\theta]_M$ is entirely negative throughout band I of P-CH=CH_2 (**2**) (Figure 2) and $B(Q_0^x)$ is positive and nearly equal in magnitude to that for OEP (Table I and Figure 6). $B(Q_0^x)$ first drops sharply to about 3×10^{-4} D^2 β_e/cm^{-1} for P-$CO_2C_2H_5$ (**3**) and the two acetyl porphyrins

(60) Stephens, P. J.; Suëtaka, W.; Schatz, P. N. *J. Chem. Phys.* **1966**, *44*, 4592.

(61) Gale, R.; McCaffery, A. J.; Rowe, M. D. *J. Chem. Soc., Dalton Trans.* **1972**, 596.

(62) Sutherland, J. C. In ref 37, Chapter 4. Figure 4 nicely illustrates how the effects of symmetric and nontotally symmetric vibrations enter differently in the absorption and in the MCD spectrum.

(63) The MCD of band IV of free-base meso tetraarylporphyrins are often bisignate. See, for example, Figures 2 and 3 of ref 27.

Table II. Comparison of B Values for the ^1L_b Transitions of Monosubstituted Benzenes and the Q_0^x Transitions of the Porphyrins

substituent	$B(^1L_b)^a$ measd[b]	$B(^1L_b)^a$ lit.[c]	$B(Q_0^x)^a$
H	0.002[d]		
CH_3	0.24	0.22[e]	
$CH{=}CH_2$	-0.35	*f*	21.61
CN	-1.91	-1.89[g]	-0.31 (**6**)
			-4.98 (**7**)
$CO_2C_2H_5$	-2.14		2.76
$COCH_3$	-2.85		3.0 (**4**)
			1.87 (**5**)
COOH	-3.43	-3.75[g]	
CHO	-3.89	-3.75[g]	-7.53

[a] 10^{-4} D^2 β_e/cm^{-1} determined from the zeroth moment for the substituted benzenes and extracted from Table I for the substituted porphyrins. [b] Isooctane. [c] *n*-Heptane. [d] Entirely vibronic. [e] Reference 5. [f] Considered to have a nonnegligible vibronic contribution (ref 7). [g] Reference 7.

(**4** and **5**), then becomes barely negative (-0.31×10^{-4} D^2 β_e/cm^{-1}) for P-CN (**6**), and finally assumes values of about -5 and -7.5 $\times 10^{-4}$ D^2 β_e/cm^{-1} for MP-CN (**7**) and P-CHO (**8**), respectively.

In terms of the actual band shaps, the MCD within band I of P-$CO_2C_2H_5$ (**3**) is monosignate (Figure 3), whereas, for similar values of $B(Q_0^x)$, the MCD for the acetyl porphyrins **4** and **5** is bisignate. Band I for the cyano porphyrins may be essentially monosignate (P-CN, **6**) or clearly bisignate (MP-CN, **7**). Finally, there is no ambiguity in the MCD associated with the Q_0^x and Q_0^y transitions of P-CHO (**8**); both are inverted compared to OEP.

Structural Aspects of the MCD of Monosubstituted Free-Base Porphyrins. In the preceding section, several consistent parallels in the effects induced by the substituents were found—most notably, the shift of the Soret absorption band maxima to lower energies (Figure 5) and the variation in the Soret MCD as measured by the peak-to-trough values[59] of bands S-I and S-II (Figure 6). In the visible region a number of seemingly aberrant effects were also found—most notably, the lack of congruency between the wavelength shifts and absorption intensity changes for the cyano porphyrins, the fuzziness of the ordering of intensity and band shifts for the ethoxycarbonyl and acetyl porphyrins, and the occurrence of sign inversion for particular members in the series.

a. Response of the Porphyrin π System to the π-Acceptor Character of the Substituents. In the preceding sections, we skirted, except in passing, specific spectral correlations with a particular measure of the electron-donating or electron-withdrawing character of the substituents themselves. In this regard, although it is of interest that the shifts in energy of the Soret transitions of the substituted porphyrins (Figure 5) and the shifts of the ^1L_a transitions of substituted benzenes[64] fall in the order of Taft's $\sigma^-_{R(g)}$ scale for π-acceptor (+E) substituents,[65] it is more relevant to utilize knowledge of MCD band sign variation in the benzene series to experimentally compare the response of the two π systems, benzene and porphyrin, to the same substituents and to provide a gauge against which to assess the structural effects commonly present for the latter π system.

Since the B values of the ^1L_b transitions for several of the substituted benzenes in the present series seem not to have been reported, values for the entire series have been determined. These values along with those for the Q_0^x transition are compared in Table II. With the exception of styrene for which vibronic effects have been cited,[7] the occurrence of parallel instances of sign inversion for the MCD of the lowest energy transitions of the two π systems would ordinarily be expected. The lack of such parallel behavior is evident from the data in Table II. Thus, the strongest (CHO) and the weakest (CN, **7**) of the π-acceptor substituents with respect to benzene both cause sign inversion in the porphyrin series, whereas the groups of intermediate character may either not ($CO_2C_2H_5$) or else only in part ($COCH_3$) evoke this response. It should be noted that, for reasons to be developed in the section "(ii) Perimeter Model," sign inversion is not necessarily expected for the Soret MCD; it is merely anticipated that changes in the intensities of the Soret MCD bands should occur.

Among the possible sources for the differences in the MCD behavior of the two π substrates are (i) the increased propensity which large π-electron systems have for aggregation, (ii) the steric interactions of the substituent groups present in the common series of substituted porphyrins but absent in the series of monosubstituted benzenes, and (iii) the unique occurrence of N-H proton tautomerism for free-base porphyrins. These structural factors will be considered in the following sections. The possibility of additional vibronic complications will be considered in a later section.

b. Aggregation as a Possible Structural Effect for Porphyrins. In the benzene series aggregation is likely to be an important factor only in the case of benzoic acid, which is known to form intermolecular hydrogen-bonded dimers in nonpolar solvents. Aggregation presents a much more serious problem for porphyrins,[66] and the additional problems imposed, particularly in the interpretation of NMR spectra, are well known for both free-base and metallo porphyrins.[67] At low temperatures, we find evidence of aggregation in, for example, the doubling of the N-H proton resonances of P-$COCH_3$ (**4**) at concentrations higher than about 7.5×10^{-4} M. In optical spectra, intermolecular association results in bisignate natural CD for the Q_0^y transitions of chlorophylls.[19] In absorption, such exciton interaction is reflected by wavelength shifts, by band broadening, and in some cases by a splitting of the Soret absorption band.[68,69a] In MCD[19,69] the spectra of associated[69a] or covalently linked[69b] porphyrins may show effects due to coupling but these appear merely to correspond to features already present in the absorption spectrum; new transitions singularly evident in the MCD spectrum do not appear to be present. We measured the MCD spectra of P-$COCH_3$ over a 100-fold concentration range (spectra were routinely measured at about 0.4×10^{-4} M) and found the shape of the Q_0^x MCD bands to be invariant. Thus, it appears that aggregation can be ruled out as a "structural effect" in the MCD of the substituted free-base porphyrins and that it will be necessary to consider electronic, structural, and vibronic effects explicitly.

c. Theoretical Models for the Interpretation of Structural Effects. For a more physical understanding of structural effects on the MCD phenomenon than is easily obtained from the full quantum mechanical expression for the B term, we return to the model presented previously in connection with the MCD of reduced porphyrins.[22] This model makes use of Michl's perturbed molecular orbital approach for understanding the occasion of sign variation among the four lowest energy purely electronic transitions of cyclic π-electron systems and Gouterman's four-orbital model of porphyrin electronic states. We adopt, initially, an intuitive approach with OEP as the reference porphyrin and then utilize INDO/S molecular orbital calculations as a way of deconvoluting the complexities of the orbital energy changes attending substitution, steric interactions with the other peripheral substituents, and the existence of N-H proton tautomerism.

(i) The Four-Orbital Model and Substituent-Induced Changes in Porphyrin Visible Absorption Spectra. In the four-orbital

(64) For a discussion and leading references, see: Jaffé, H. H.; Orchin, M. "Theory and Applications of Ultraviolet Spectroscopy"; Wiley: New York, 1962; pp 256–259.

(65) Reynolds, W. F.; Dais, P.; MacIntyre, D. W.; Topson, R. D.; Marriott, S.; Nagy-Felsobuki, E. V.; Taft, R. W. *J. Am. Chem. Soc.* **1983**, *105*, 378. $\sigma^-_{R(g)}$ = 0.45, 0.43, 0.41, and 0.23 for CHO, CH_3CO, CO_2CH_3, and CN, respectively. The inductive parameter $\sigma_{I(g)}$ runs in a different order: 0.58, 0.31, 0.22, 0.17 for CN, CHO, $COCH_3$, and CO_2CH_3, respectively.

(66) White, W. I. In "The Porphyrins"; Dolphin, D., Ed.; Academic Press: New York, 1978; Vol. V, Chapter 7.

(67) (a) Janson, T. R.; Katz, J. J. In "The Porphyrins"; Dolphin, D., Ed.; Academic Press: New York, 1979; Vol. IV, Chapter 1. (b) Abraham, R. J.; Fell, S. C. M.; Pearson, H.; Smith, K. M. *Tetrahedron* **1979**, *35*, 1759.

(68) Selensky, R.; Holten, D.; Windsor, M. W.; Paine, J. B., III; Dolphin, D.; Gouterman, M.; Thomas, J. C. *Chem. Phys.* **1981**, *60*, 33.

(69) (a) Reimer, K. J.; Reimer, M. M.; Stillman, M. J. *Can. J. Chem.* **1981**, *59*, 1388. (b) Collman, J. P.; Basolo, F.; Bunnenberg, E.; Collins, T. J.; Dawson, J. H.; Ellis, P. E.; Marrocco, M. L.; Moscowitz, A.; Sessler, J. L.; Szymanski, T. *J. Am. Chem. Soc.* **1981**, *103*, 5636.

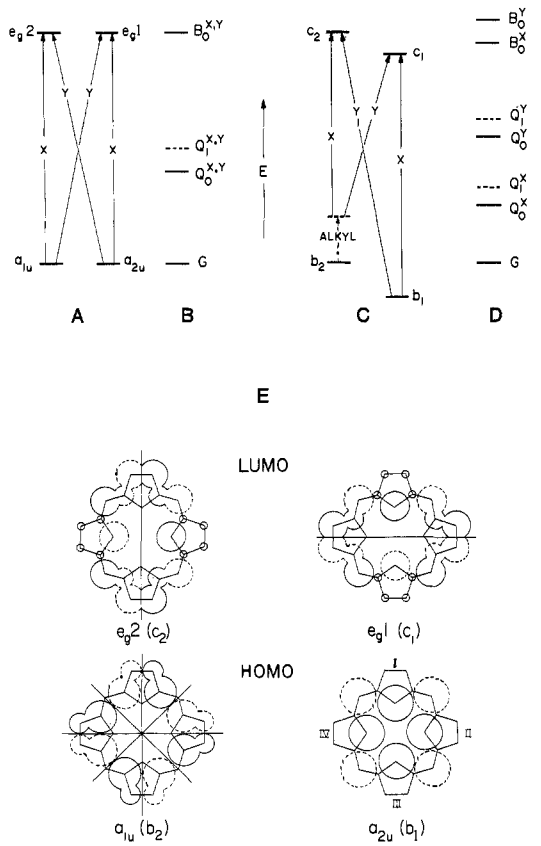

Figure 7. (A and B) Four-orbital and state energy level diagrams for the reference D_{4h} porphyrin, porphine dianion, respectively. (C and D) Four-orbital and state energy level diagrams for a reference D_{2h} porphyrin, porphine free-base. Protons are placed along the vertical axis (defined to be the x axis). The principal effect of octaalkyl substitution is indicated by the dashed line and arrow. (E) Porphine HOMO and LUMO orbitals redrawn from ref 41a. The sizes of the circles are proportional to the squares of the atomic orbital coefficients. The orbital symmetry labels a_{1u}, a_{2u}, e_g2, and e_g1 are appropriate for D_{4h} porphyrins. Their corresponding descendants for porphyrins of lower symmetry are labeled b_2, b_1, c_2, and c_1.

model,[41] low-lying porphyrin $\pi\pi^*$ states are pictured as arising from single electron excitations from a pair of HOMO's to a pair of LUMO's (Figure 7). For a D_{4h} porphyrin (Figure 7A) the LUMO's (e_g1 and e_g2) are degenerate by symmetry and the HOMO's are taken to be accidentally degenerate as well. Excitation gives rise to a pair of doubly degenerate singlet configurations, $^1(a_{2u}e_g)$ and $^1(a_{1u}e_g)$, which undergo strong configuration interaction to yield the separately degenerate B (Soret) and Q states (Figure 7B). In the Soret state the electric transition dipoles add whereas in the Q state they subtract. Thus, the Soret states of D_{4h} porphyrins have large dipole strengths associated with them while transitions into the Q states are quite weak and vanish if the HOMO degeneracy is exact, as is nearly the case for porphine dianion.[26] Conversely, the magnetic transition dipoles add for the Q state but subtract for the Soret state. As a result, transitions into the Q states of D_{4h} porphyrins have sizable magnetic moments associated with them ($\sim$3–5 β_e) whereas those of transitions into the Soret states are much smaller ($\sim$0.3 β_e).[60,61] Here, we will utilize Michl's nomenclature[15] and will refer to the magnetic moment of the Q state as μ^+ and that of the Soret state as μ^-.

When two protons are placed on opposed nitrogens to form trans free-base porphine, the symmetry-imposed degeneracy of the LUMO's and the accidental degeneracy of the HOMO's of porphine dianion are lifted (Figure 7C).[70] The ordering of the c_1 and c_2 orbitals is determined by the placement of the protons (here the vertical axis is chosen as the x axis) and the relative splitting of the HOMO and LUMO orbitals (ΔHOMO > ΔLUMO) is a consequence of the inductive electron-withdrawing effect of the protons on both the HOMO and LUMO orbitals and the difference in the magnitudes of the squares of the atomic orbital coefficients for the nitrogens in the affected orbitals (c_1 and b_1, Figure 7E). Because of the D_{2h} symmetry of the free base, the electric transition dipoles in the x and y directions are no longer equivalent and substantial splitting in the energy levels of the Q_0^x and Q_0^y states occurs (Figure 7D). The four-orbital Soret states (B_0^x and B_0^y) are also split, but by a much smaller amount.[41,61]

The four-orbital model of porphyrin electronic states outlined above has been of enormous value to porphyrin chemists and spectroscopists as a first-order, highly intuitive approach for understanding porphyrin electronic structure and spectra, and its general validity for the Q states has been supported by a number of calculations.[39,41c] It does not, however, describe the Soret region well since more than the two B_0^x and B_0^y states allowed by the four-orbital model are often clearly evident in the MCD spectrum and in calculations.[39] The latter are not, however, a matter of focus in our present work which deals primarily with the absorption and MCD of the visible transitions.

Since we have examined the effects of the CH=CH$_2$, CO$_2$C$_2$H$_5$, COCH$_3$, CN, and CHO substituents on the electronic absorption spectra of free-base porphyrins in some detail in preceding sections, it is pertinent to follow here the very simple perturbation arguments presented by Gouterman in his first formal four-orbital model paper.[41a] Gouterman noted that the amount of absorption intensity gained in the Q_0^x and Q_0^y transitions of any free-base porphyrin by borrowing from the appropriate Soret states can be related to the difference in orbital energies of the states reached by x and y singlet electron excitations, respectively. Thus, in the orbital energy level diagram for porphine free-base (the solid lines in Figure 7C), $[E(c_2) - E(b_2)] \approx [E(c_1) - E(b_1)]$ for the x-polarized excitations and $[E(c_2) - E(b_1)] \approx [E(c_1) - E(b_2)]$ for the y-polarized excitations. The consequence of these near equalities of the orbital energy differences for free-base porphine itself is that its Q_0^x and Q_0^y transitions should be quite weak as is actually the case (see Figure 2, ref 22a). Since alkyl groups behave as mesomeric electron-donating (–E) substituents,[10,56] the dominant effect of octaalkyl substitution at the pyrrole positions as for OEP (**1**) is to raise the energy of the b_2 orbital as is indicated by the broken arrow in Figure 7C. As a consequence of this alkyl-substituent-induced orbital energy shift, the energy differences between the respective x and y excitations are no longer approximately equal and an increased amount of dipole strength in both the Q_0^x and Q_0^y transitions of OEP (Figure 2) is gained by borrowing from the B_0^x and B_0^y states, respectively. In terms of ϵ_{max}'s the ratios octaethylporphyrin-to-porphine are about 6 and 4.3 for the Q_0^x and Q_0^y transitions, respectively.

It is particularly relevant to note that this simple perturbation treatment provides a very satisfying way of understanding the principal changes in the absorption spectra which occur in the series of monosubstituted porphyrins. For simplicity, we restrict our attention to a single tautomeric form and consider the diagram (Figure 7C) modified for an octaalkyl reference porphyrin. Notice that if the protons are placed along the vertical (x) axis and if a π-acceptor substituent is placed on a pyrrole ring which does not bear an internal proton (e.g., ring II), then the dominant effect of the substituent (not shown in Figure 7C; see Figure 8C and discussion) is to lower the energy of the c_1 orbital. For a relatively weak π-acceptor substituent such as the CN group, the effect is to cause the orbital energy differences for the x-polarized excitations to become almost the same while the energy differences for the y-polarized excitations become larger. This is the point at which the strength of the Q_0^y transition increases while that of the Q_0^x transition almost vanishes. This relative energy change is accompanied by only small changes in total configurational energies. Consequently, large visible band absorption intensity changes occur but with minimal shifts in transition energies. Thus, the two seemingly conflicting events in the absorption spectra of the cyano porphyrins commented on in the preceding sections can be accounted for on the basis of a naive application of the four-

(70) The cis N–H tautomer may ultimately need to be considered for particular free-base porphyrins.

orbital model. It does not, however, directly account for the doubling of absorption bands I evident in the spectra of the cyano porphyrins (Figure 4). For this we will later consider tautomerism and vibronic effects. The model also accounts for the changes observed in the absorption spectra of the other substituted porphyrins. For instance, the formyl group is a stronger π-acceptor than the cyano group. Its principal effect is to lower the energy of the c_1 orbital even further, past the point of near equality in the energies of the x-polarized excitations. Thus, the dipole strength for the Q_0^x transition of P-CHO is larger than the total dipole strength for band I of the cyano porphyrins (Table I). Correspondingly, the larger orbital energy shifts produced by the formyl group result in larger configurational energy changes, and the transitions for P-CHO are shifted more than are those of P-CN or MP-CN. The other π-acceptor groups ($CO_2C_2H_5$ and $COCH_3$) affect the orbital energies in ways that are mediated by their intrinsic and effective (steric) π-acceptor strengths. Finally, the vinyl group as a weak $\pm$E substituent lowers the energy of the c_1 orbital somewhat but also raises the energy of the b_2 orbital. This balance results in only minor dipole strength changes but does cause the transitions to undergo small red shifts.

(ii) **The Perimeter Model.** Michl's perimeter model has come to occupy a position analogous to that of Gouterman's four-orbital model for porphyrin electronic states in that it provides a very useful, intuitively appealing, first-order approach for relating the absolute signs of the four lowest energy purely electronic MCD bands associated with π–π^* transitions of cyclic π-electron systems to their molecular structures. It has been presented in detail[15] and reviewed[16] by Michl, and some aspects of it which are pertinent to porphyrin electronic structure determination have been presented[22b] and elaborated for specific problems.[26b,27]

The assertion made in the perimeter model is that in many cases the occurrence of sign variation in relevant molecular systems can be understood quite simply in terms of the relative magnitudes of the orbital energy differences between the two highest occupied (ΔHOMO, $|E(b_2) - E(b_1)|$ in Figures 7C and 8C) and the two lowest unoccupied (ΔLUMO, $|E(c_2) - E(c_1)|$) molecular orbitals. For porphyrins of symmetry lower than D_{4h}, three orbital energy dispositions may occur which are pertinent to the sign patterns that may be observed in the MCD spectrum. When ΔHOMO = ΔLUMO, MCD intensity in the Soret transitions arises from intrastate (B_0^x, B_0^y) mixing, and MCD intensity in the visible region transitions is due only to interstate ($Q_0^{x,y}$, $B_0^{x,y}$) mixing. The operative magnetic moment is the μ^- moment of the Soret state which is small and negative for cyclic π-electron systems like porphyrins.[15a] The MCD associated with μ^- contributions is not particularly sensitive to structure; furthermore, since the μ^- moment is small and since MCD intensity is scaled according to the reciprocal of the differences in the energies of the states mixed by the magnetic field, the MCD which arises in this way is small at best for the lowest energy states (and will be ignored here) but quite significant for the higher energy Soret states.

More important for structural effect correlations are the potentially large μ^+ contributions of the Q state magnetic moment which arise when the equality between ΔHOMO and ΔLUMO breaks down. If ΔHOMO < ΔLUMO, which is the condition of particular interest here, then the overall $[\theta]_M$ sign pattern potentially imposed on the four lowest energy purely electronic MCD bands is +−+− in the order of increasing energy. However, whether this complete pattern is actually observed in an MCD spectrum depends critically on the magnitude of |ΔHOMO − ΔLUMO|. For relatively small values, sign inversion (i.e., the $[\theta]_M$ pattern +−) occurs first for the Q_0^x and Q_0^y transitions. In the Soret MCD bands the effect of the μ^+ contribution is felt first as a diminution in the intensities of the MCD bands (e.g., see the MCD spectrum of P-CHO in Figure 4), and it is only for quite large values of |ΔHOMO − ΔLUMO| that the fully inverted MCD band sign pattern +−+− can be expected to occur for all four bands. On the other hand, when the structure of the porphyrin imposes the orbital energy condition ΔHOMO > ΔLUMO, the μ^+ contribution to the MCD of Q_0^x and Q_0^y transitions is −+, and the same −+ contribution to the Soret MCD bands merely reinforces that of the structurally invariant μ^- contribution (−+). The resulting overall sign pattern of −+−+ is occasionally referred to as the "normal" sign pattern.[18,22]

d. Structural Features of Substituted Free-Base Porphyrins. The MCD that is actually observed (Figures 2–4) arises from all of the molecular species present in the solution. Thus, the occurrence of sign variation for free-base porphyrins is governed by the π-acceptor character of the substituent, by the way in which steric interactions influence mutual overlap of the constituent porphyrin and substituent π orbitals, and by modulations in the splitting of the LUMO's due to N–H proton tautomerism.

(i) **Stereochemistry of Porphyrin Substituents.** The conformational equilibria shown in Figure 8A illustrate the range of conformer species which we propose contribute in some degree to the observed MCD and absorption spectra of the vinyl- and carbonyl-substituted porphyrins. The cyano group is cylindrically symmetric and can be excluded from this consideration. In conformer **9a**, the functionality Y (CH_2 or O) is directed toward the adjacent methyl group whereas the functionality R (H, CH_3, or OC_2H_5) is directed toward the adjacent meso hydrogen. Conversely, for conformer **9b**, Y is near the meso hydrogen and R is near the adjacent methyl group. Steric interactions of Y or R with either the meso hydrogen or the methyl group can impede the attainment of maximum overlap of the substituent's π orbitals with those of the porphyrin ring and can thereby influence the spectroscopic behavior of the substituted porphyrin to a greater or lesser extent depending on the steric bulk inherent to the chromophoric group. Rotational transition between these two extreme forms is gained via conformer **10** for which the orthogonality of the two π systems precludes resonance interaction, leaving then only inductive effects which are usually less important[15,16] for MCD band sign variation.

Relatively little definitive information about the solution stereochemistries of porphyrin chromophoric substituents is available in the literature. In the solid state the vinyl groups of protoporphyrin IX dimethyl ester point toward the adjacent methyl groups (**9a**) but are held 20° out of the plane of the porphyrin ring because of steric constraints.[71a] In solution, ^{1}H NMR measurements of biscyano iron(III) protoporphyrin IX dimethyl ester[71b] as well as ^{1}H NMR[71c] and resonance Raman (RR)[71d,e] measurements of heme proteins are consistent with large rotational mobilities and out-of-plane conformations for the vinyl group. In the solid state, the acetyl groups of nickel(II) 2,4-diacetyldeuteroporphyrin IX dimethyl ester point, in contrast to the case of vinyl groups, toward the meso hydrogens and away from the methyl groups (**9b**)[72a] and are out of the porphyrin plane by 3 and 17°. The ^{13}C NMR spectrum of the free base is also consistent with these directional orientations.[72b] The recent crystal structure determination of a diformyl porphyrin[73a] shows that, like the acetyl group, the oxygen atoms of the formyl groups point toward the meso hydrogens (**9b**) and are nearly coincident (~5°) with the plane of the porphyrin ring. This directional orientation is consistent with results of ^{13}C NMR measurements on a formyl-substituted chlorin derivative,[73b] and RR measurements of the formyl-substituted heme *a* contained in cytochrome *c* oxidase[73c,d] indicate that appreciable π-overlap persists in solution. No information on the stereochemistry of nuclear carboxylic ester groups seems to have been reported; however, space-filling molecular models indicate that the effective steric bulk of the ethoxycarbonyl group exceeds that of the acetyl group and thus conformations

(71) (a) Cauchey, W. S.; Ibers, J. A. *J. Am. Chem. Soc.* **1977**, *99*, 6639. (b) LaMar, G. N.; Viscio, D. B.; Gersonde, K.; Sick, H. *Biochemistry* **1978**, *17*, 361. (c) Satterlee, J. D.; Erman, J. E. *J. Biol. Chem.* **1983**, *258*, 1050. (d) Rousseau, D. L.; Ondrias, M. R.; LaMar, G. N.; Kong, S. B.; Smith, K. M. *Ibid.* **1983**, *258*, 1740. (e) Shelnutt, J. A.; Satterlee, J. D. *Ibid.* **1983**, *258*, 2168.

(72) (a) Hamor, T. A.; Caughey, W. S.; Hoard, J. L. *J. Am. Chem. Soc.* **1965**, *87*, 2305. (b) Doddrell, D.; Caughey, W. S. *Ibid.* **1972**, *94*, 2510.

(73) (a) Chang, C. K.; Hatada, M. H.; Tulinsky, A. *J. Chem. Soc., Perkin Trans. 2* **1983**, 371. (b) Lincoln, D. N.; Wray, V.; Brockmann, H.; Trowitzsch, W. *Ibid.* **1974**, 1920. (c) Tsubaki, M.; Nagai, K.; Kitagawa, T. *Biochemistry* **1980**, *19*, 379. (d) Babcock, G. T.; Salmeen, I. *Ibid.* **1979**, *18*, 2493.

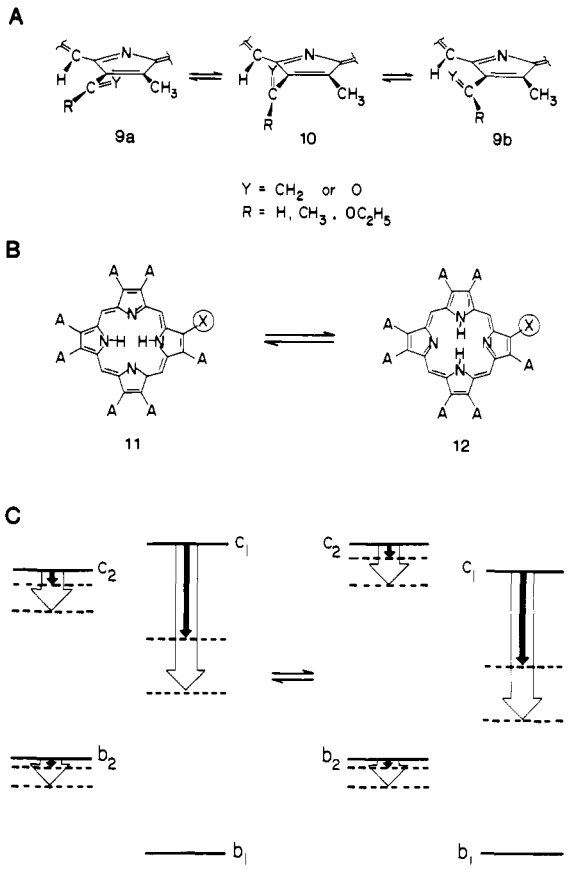

Figure 8. (A) A representation of the equilibria between substituent group conformer populations contributing to the observed absorption and MCD spectra of the monosubstituted porphyrins. The cyano group is cylindrically symmetric and has no conformational contribution. (B) Equilibria between the trans N–H proton tautomers of the substituted porphyrins. "A" represents any alkyl or alkyl-like substituent. "X" is any one of the chromophoric substituents mentioned in the text, including the cyano group. The conformer and tautomer equilibria are not independent. (C) A schematic representation of the HOMO and LUMO energy level diagrams for the "horizontal" and "vertical" N–H proton tautomers of the reference porphyrin OEP (1) (solid lines) and the energy levels reached owing to substitution of a single electron-withdrawing substituent (dashed lines). The large arrows represent the effects of a strong electron-withdrawing substituent such as CHO. The smaller arrows represent the effects of a weaker substituent. The effect of the vinyl group is not indicated, but is discussed in the text. The proton axis is taken as the x axis for both tautomers.

like that of **10** should make important contributions to P-$CO_2C_2H_5$.

(ii) N–H Proton Tautomerism. The equilibrium represented in Figure 8B illustrates the second structural effect which complicates the interpretation of the electronic absorption and MCD spectra of substituted free-base porphyrins. The question of the location of the internal protons of free-base porphyrins and the dynamics of their migration, which is known to be rapid on the NMR time scale at room temperature,[74a] has been the subject of a large number of investigations utilizing a broad spectrum of physical techniques including X-ray diffraction,[74b] IR,[74c,d] X-ray PES,[74e] ^{1}H NMR,[74f] ^{13}C NMR,[74g] ^{15}N NMR,[74h] photochemical hole-burning,[74i] and fluorescence and fluorescence polarization spectroscopy.[74j,k] Although there is continuing interest in the mechanism of the proton migration,[74l] there is little doubt that for symmetrically substituted porphyrins the trans tautomers are more stable than the cis tautomers. There is no direct experimental[75] knowledge, however, of the internal proton distributions for free-base porphyrins which bear electron-withdrawing substituents at peripheral positions (except for the recent crystal structure determination of a porphyrin having formyl substituents on opposed pyrrole rings[73a]). Here, we restrict our attention to the trans forms (**11** and **12**, Figure 8B).

e. Interpretation of the Interaction between Tautomeric and Steric Effects on the MCD of Monosubstituted Porphyrins. The diagrams in Figure 8C illustrate in schematic form the way in which we propose the conjunctive effects of N–H proton tautomerism and the effective π-acceptor character of the substituents affect the energies of the four frontier porphyrin molecular orbitals and so, in the context of Michl's perimeter model, influence the occurrence of MCD band sign variation.

The energy levels for the "horizontal" tautomer of an octaalkyl porphyrin such as OEP (**11**, X = A = C_2H_5) are depicted on the left side of Figure 8C by solid lines and those of the "vertical" tautomer are shown on the right side.[76] The proton axis is chosen to be the x axis in both cases. Notice that only the ordering of the LUMO's (c_2 and c_1) depends on whether the protons are placed along the horizontal or along the vertical axes. Thus, $|\Delta\text{HOMO} - \Delta\text{LUMO}|$ is the same for the trans tautomers of OEP and they exhibit identical MCD as well as absorption spectra. This will not be the case for the substituted porphyrins.

Each of the π-acceptor substituents (CN, $CO_2C_2H_5$, $COCH_3$, and CHO) has unfilled π^* orbitals which can interact more strongly[56] with the porphyrin LUMO's than with the porphyrin HOMO's, and the extent to which the energy of an orbital is lowered depends on the square of the AO coefficient at the point of attachment and on the π-acceptor character of the particular substituent. The squares of the AO coefficients are represented by circles of varying size in Figure 7E. Thus, the energy of the c_1 LUMO is the most strongly affected, followed by that of the c_2 LUMO, and then that of the b_2 HOMO. Substituents at the pyrrole positions have very little effect on the energies of the b_1 orbital and none is indicated in Figure 8C. Arrows of different size are used to indicate two extremes of substituent π-acceptor capability.

Several important general features are expressed in Figure 8C. (i) While the trans distribution of the internal protons is immaterial for determining the MCD of OEP (**1**), the position of the protons could, *in principle*, be a major factor in determining the MCD spectrum of a substituted porphyrin. This would be especially the case for a relatively weakly perturbing substituent (due either to its intrinsic π-acceptor character or to its effective electron-withdrawing character caused by steric constraints) as is indicated by the darkened arrows since if **11** and **12** were equally populated, the energy level diagrams for such a substituent in Figure 8C indicate that $\Delta\text{HOMO} > \Delta\text{LUMO}$ for the horizontal tautomer (**11**) but that $\Delta\text{HOMO} < \Delta\text{LUMO}$ for the vertical tautomer (**12**). The former would exhibit the normal $-+$ ($[\theta]_M$) sign pattern for the MCD bands associated with the Q_0^x and Q_0^y transitions, respectively, whereas the latter would exhibit the inverted $+-$ sign pattern for these transitions. Since all molecular species present are effectively observed in an optical spectrum, each with its own characteristic excitation energies, the distribution of tautomeric species could affect the shape of the MCD spectrum. However, whether bisignate MCD would necessarily be observed depends

(74) (a) The lifetime of a tautomer is estimated to be about 10^{-2}–10^{-3} s at room temperature and several hours at 77 K. (b) Lauher, J. W.; Ibers, J. A. *J. Am. Chem. Soc.* **1973**, *95*, 5148. (c) Mason, S. F. *J. Chem. Soc.* **1958**, 976. (d) Limbach, H. H.; Hennig, J.; Stulz, J. *J. Chem. Phys.* **1983**, *78*, 5432. (e) Niwa, Y.; Kobayashi, H.; Tsuchiya, T. *Ibid.* **1974**, *60*, 799. (f) Storm, C. B.; Teklu, Y. *J. Am. Chem. Soc.* **1972**, *94*, 1745. (g) Abraham, R. J.; Hawkes, G. E.; Hudson, M. F.; Smith, K. M. *J. Chem. Soc., Perkin Trans. 1* **1975**, 204. (h) Kyogoku, Y. *Appl. Spectrosc. Rev.* **1981**, *17*, 279. (i) Thijssen, H. P. H.; Dicker, A. I. M.; Völker, S. *Chem. Phys. Lett.* **1982**, *92*, 7. (j) Gurinovich, G. P.; Sevchenko, A. N.; Solov'ev, K. N. *Opt. Spectrosc.* **1961**, *10*, 396. (k) Gouterman, M.; Stryer, L. *J. Chem. Phys.* **1962**, *37*, 2260. (l) Hennig, J.; Limbach, H. H. *J. Am. Chem. Soc.* **1984**, *106*, 292.

(75) The optical spectra of the cis and trans tautomers of porphine have recently been calculated with INDO/S: Rawlings, D. C.; Davidson, E. R.; Gouterman, M. *Theor. Chim. Acta* **1982**, *61*, 227.

(76) It is difficult to accurately represent the relative splitting of the HOMO and LUMO orbitals of an octaalkyl porphyrin, since estimates of these values are available only from calculations on unsubstituted porphine and these values are in any case model-dependent (e.g., in ref 77 $\Delta\text{HOMO}/\Delta\text{LUMO} = 6.6$, whereas in ref 39 the ratio is 17). Comparison of both the absorption and MCD spectra of OEP and porphine (see text) suggests that the ratio should be larger for OEP than that calculated for porphine itself.

Table III. MCD and Absorption Spectral Data for Band I of Monosubstituted Free-Base Porphyrins in Dichloromethane at 295 and 199 K

compound[a]	temp (K)	absorption[b] $\lambda_{max}(10^{-3}\epsilon)/D$[c]	absorption[b] $\Delta D/(\%)$[d]	MCD[b] λ_{max} $([\theta]_M)/10^{-4}B$[e]	MCD[b] $\Delta B/(\%)$[f]
OEP (1)	295	619 (4.6) 0.96		617 (−3.0) {21.26}	
	199	615 (4.6) 0.79	−0.17 (−18)	613 (−3.2) {19.09}	−2.17 (−10)
P-CH=CH_2 (2)	295	625 (4.0) 1.01		625 (−2.8) {22.89}	
	199	622 (4.1) 0.88	−0.13 (−13)	621 (−3.3) {23.06}	+0.17 (+0.7)
P-$CO_2C_2H_5$ (3)	295	633 (2.3) 0.62		622 (−0.3) {2.76}	
	199	631 (1.6) 0.40	−0.22 (−35)	?[g] ~0	−2.76 (−100)
P-$COCH_3$ (4)	295	634 (1.6) 0.53		621 (−0.6) 636 (0.2) {4.74} {−0.81} B_{total} = 3.93	
	199	630 (1.4) 0.26	−0.27 (−51)	614 (−0.3) 626 (0.6) {1.76} {−3.17} B_{total} = −1.41	−5.34 (−136)
P-CN (6)	295	623 (0.6)[h] 0.26		606 (−0.1) 631 (0.4) {0.87} {−2.55} B_{total} = −1.68	
	199	618 (0.8)[h] 0.31	+0.05 (+19)	626 (1.2) {−7.40}	−5.72 (−340)
MP-CN (7)	295	622 (0.7)[h] 0.28		602 (−0.1) 624 (0.9) {~0.2} {−6.12} B_{total} = −5.90	
	199	618 (0.9) 0.31	+0.03 (+11)	621 (1.4) {−9.59}	−3.69 (−62)
P-CHO (8)	295	637 (1.3) 0.43		634 (1.1) {−8.15}	
	199	631 (0.9) 0.28	−0.15 (−35)	631 (1.7) {−13.51}	−5.36 (−66)

[a] Structures are given in Figure 1. [b] A factor of 1.15 has been used to allow for the decrease in volume of CH_2Cl_2 at 199 K. In several cases the concentration of the porphyrin was determined from the Soret extinction coefficient of the porphyrin in $CHCl_3$. Units of measurement are given in footnotes *c* and *d* of Table I. [c] Values for the dipole strength, *D*, were extracted by a full-band curve-fitting protocol which was also the basis for the unenclosed values in Table I. [d] Change and percent relative change in the dipole strength with respect to the initial (295 K) measurements; thus, a negative sign indicates a decrease in *D*. [e] Values for the *B* term were obtained from the zeroth moment and thus again correspond to the values enclosed within braces in Table I. [f] Change and percent relative change in the *B* value with respect to the initial (295 K) measurement; thus, a negative sign indicates that *B* becomes less positive at the lower temperature. [g] MCD is within the noise level of the measurement; however, $[\theta]_M$ may be slightly positive around 624 nm and slightly negative around 610 nm. [h] Fitted as a single broad absorption band in contrast to the two-band curve-fit data given in Table I. λ_{max} is the maximum of the fitted band. ϵ_{max} is the value for the stronger of the two components (see expansion plot in Figure 4).

on the values of |ΔHOMO − ΔLUMO| for the two tautomeric species and on the separation in transition energies of the two forms. The effects of tautomerism for a much stronger π-acceptor, even under the condition of equal population of **11** and **12**, could well be much less dramatic since, as indicated by the open arrows in Figure 8C, the orbital energies could be such that ΔHOMO < ΔLUMO for either tautomer. This situation would result in the occurrence of sign inversion for both forms. (ii) Again for a fixed but now nonspecific distributions of tautomers (**11** and **12**), the presence of more than one substituent group conformer population could also have a major effect on the MCD, and concomitantly the absorption, spectrum of a substituted porphyrin since in the populations (represented by structures **9a** and **9b**) for which π orbital overlap is the maximum accorded by steric constraints, the substituent would have the π-acceptor character of a strongly perturbing group, whereas in the populations represented roughly by structure **10** for which π orbital overlap is minimal, the substituent would have a much weaker +E effect. Populations like **9a** and **9b** would then be expected to exhibit sign inversion whereas those like **10** should show the normal sign pattern.[77] The possibility of actually observing bisignate MCD would again depend on the values of |ΔHOMO − ΔLUMO| and on the energies of the transitions of the species present. (iii) Although experimental evidence is lacking (see the section: (ii) N−H Proton Tautomerism, above), it is unlikely that the tautomers **11** and **12** are equally populated even in solutions of the substituted free-base porphyrins at room temperature since electron withdrawal by the substituent influences the electron density on the nitrogens.

From what has been said, it is clear that an understanding of the effects of single substituents on the MCD and absorption spectra of free-base porphyrins is complicated by the possible presence of both steric and tautomeric effects and that this is likely to be further complicated by the incursion of vibronic effects (vide infra). In principle, several means are at hand for at least partially disentagling these effects. (i) Explicit calculations of the energies of the pertinent four frontier molecular orbitals can be used to track the electronic effects of steric and tautomeric interactions (see a following section). (ii) Experimentally, it may be possible to emphasize tautomeric and structural effects respectively by the synthesis of separate series of sterically unhindered and sterically more hindered substituted porphyrins. Such synthetic work is presently in progress.[42] (iii) The tautomer aspect of the problem can be removed by the insertion of metals into the porphyrin core. The conclusions from preliminary work along these lines are consistent with the general inferences about the π-acceptor character of the substituents made here. However, the extraction of unambiguous information about substituent group conformer equilibria is complicated by the near degeneracy of the electronic transitions and by the presence of nearby vibrational bands. (iv) The effects of temperature variation on the MCD and absorption spectra of the substituted free-base porphyrins themselves can be examined with the view that the spectral changes observed for the sterically unhindered cyano and less hindered formyl porphyrins may provide information from which to judge the general

(77) For reasons of simplicity, we consider **9a** or **9b** and **10** as two extremes of substituent orientation. In a particular case, either **9a** or **9b** could give rise to uninverted spectra.

importance of that portion of the LUMO splitting which is due to N–H tautomerism.

Here the temperature variations observed for the Q_0^x MCD and absorption bands (Table III) along with specific spectral features form the basis for some summarizing remarks on the electronic aspects of the problem. In connection with Figure 8, it should be noted that at lower temperatures the populations of the vertical tautomer species (**12**) and the populations of the more coplanar conformer species (**9a** and **9b**) are expected to increase. Consequently, the level diagrams on the right-hand side of Figure 8C should then become the more applicable ones. Since these are the ones which favor the condition $\Delta HOMO < \Delta LUMO$, occasions for the occurrence of MCD band sign inversion are favored at lower temperature.

(i) **Vinyl Group.** Whether the π-acceptor (+E) or π-donor (–E) character of the ±E vinyl group dominates depends on the π system to which it is attached.[56] If not of vibronic origin,[7] the occurrence of a negative *B* term for the ^1L_b transition of styrene (Table II) suggests that its +E nature may be somewhat preferred for that system. (Note in Table II that the methyl group, a weak –E substituent, gives rise to a negative *B* term for the ^1L_b transition of toluene.) For the porphyrin π system, its ±E character seems more balanced—its dominant effect (not shown in Figure 8) being to lower and raise the energies of the c_1 and b_2 orbitals, respectively, by about the same amounts, thereby affecting the energies of the transitions (Figures 2 and 5) but leaving the condition $\Delta HOMO > \Delta LUMO$ unchanged and thus precluding the occurrence of MCD band sign inversion. At lower temperatures, the populations of conformers like **9a** and **9b** should increase and a slight shift in the tautomer distribution may also occur; however, as the data for P-CH=CH_2 in Table III indicate, the changes in the spectra are quite small, in fact, less than those observed for OEP. In both cases (**1** and **2**), the Q_0^x transition shifts to somewhat higher energies at the lower temperature.[78]

(ii) **Cyano Group.** According to the parameters of Taft (see ref 65), the cyano group is the weakest of the +E substituents but, conversely, its +I effect is the strongest, by far, of all the substituents studied. As a +E substituent, its dominant effect is to lower the energy of the c_1 orbital (Figure 8C), whereas as a +I substituent, its principal effects are to lower the energies of both the c_1 and the b_2 orbitals. The two effects, +E and +I, thus operate in the same direction in the sense of favoring the condition $\Delta HOMO < \Delta LUMO$. It causes sign inversion in the ^1L_b benzene transition, but it is not the most strongly perturbing benzene substituent (Table II) and, judging by the small red shifts it evokes in the energies of the porphyrin absorption bands (Figure 5) and by its minimal effects on the porphyrin Soret MCD band intensities (Figure 6), it has a relatively weak effect on this π system as well. It does, however, evoke major changes in the intensities of the Q_0^x (accompanied by band doubling, Figure 4) and Q_0^y transitions which find a natural explanation in terms of Gouterman's four-orbital model (vide supra) and, in addition, bisignate MCD is associated with both the Q_0^x and Q_0^y transitions of the cyano porphyrins, especially for **6** (Figure 4). At low temperature the absorption band associated with the long-wavelength shoulder of band I appears to blue shift under the envelope of the second transition in that the total dipole strength of band I increases for both P-CN and MP-CN at 199 K (Table III). Concurrently, the bisignate characteristics present for the MCD associated with band I of either P-CN or MP-CN at room temperature vanish and the MCD becomes entirely positive.

An explanation *biased toward structure effects* which is generally consistent with these observations is that the spectra of the cyano porphyrins reflect the presence of two tautomeric species (**11** and **12**). In the energy level diagrams of Figure 8C the horizontal tautomeric (**11**) forms of the cyano porphyrins are represented by the darkened arrows in the left-hand diagram, whereas the vertical tautomers (**12**) are shown by the darkened arrows on the right side. The former are then presumed to give rise to the negative MCD bands ($\Delta HOMO > \Delta LUMO$) observed for P-CN and MP-CN in Figure 4 and presumably to one of the absorption bands, whereas the latter give rise to the positive portions of the MCD (since for them $\Delta HOMO < \Delta LUMO$) of band I and to the second of the two absorption bands. Lowering the temperature should then shift the tautomeric equilibria for the cyano porphyrins to the right with the consequence that at low temperature only positive MCD is observed (Table III). These might be compelling arguments that we are indeed exclusively observing the effects of N–H proton tautomerism were it not for the fact that the MCD associated with band I of the two cyano porphyrins is markedly different. This event is disturbing with regard to an unambiguous structural interpretation and requires that we consider vibronic effects in more detail (vide infra).

(iii) **Ethoxycarbonyl Group.** The carboxylic ester group is a better π-acceptor than the cyano group when attached to the benzene π substrate (Table II), and this appears also to be the case when it is attached to the porphyrin ring from the band shift data (Figure 5) and the Soret MCD PT values (Figure 6). In contrast, however, to the benzene series (Table II), the ethoxycarbonyl group does not evoke sign inversion in the MCD of the lowest energy porphyrin electronic transitions (Figure 3).

A structural explanation for this event is that while conformer and tautomer species (**9a** or **9b** and **12**) may be present which, in the limit, could give rise to the orbital energy situation illustrated on the right side of Figure 8C wherein $\Delta HOMO < \Delta LUMO$ and thus to sign inversion, the steric bulk of the $CO_2C_2H_5$ group is sufficiently large that conformer species such as **10** are highly populated. For them, $\Delta HOMO > \Delta LUMO$ (left side of Figure 8C) and the positive *B* term observed for band I and the negative *B* term for band III (Figure 3) would be expected. For the solution stereochemistry of the ethoxycarbonyl group we have proposed (approximated by structure **10**), it might also be expected that the two tautomeric forms, **11** and **12**, would be similarly populated. Lowering the temperature should then affect both equilibria in a conjunctive manner with the result that the orbital energy disposition depicted on the right side of Figure 8C should be more favored. The data given in Table III for P-$CO_2C_2H_5$ indicate that the temperature-dependent orbital energy shifts proposed are indeed in the right direction since the MCD associated with the Q_0^x transition essentially vanishes (footnote *g*, Table III) at 199 K. Finally, because of the relatively narrow range of spectrally distinguishable species proposed, the shapes of the MCD and absorption bands associated with band I should be rather symmetrical (Figure 3) and well-defined (compare the FB and TLE fitted and moment data in Table I). The absorption band symmetry is maintained at low temperature while the dipole strength decreases.

(iv) **Acetyl Group.** The acetyl group is distinguished from the ethoxycarbonyl group by its stronger π-acceptor character with respect to both the benzene (Table II) and porphyrin (Figures 5 and 6) π systems and by its smaller effective steric bulk. A consequence of both of these factors is that the MCD associated with the Q_0^x transitions of the acetyl porphyrins P-$COCH_3$ and DP-2-$COCH_3$ (**4** and **5**) (Table I, Figure 3) is partially inverted in sign.

We suggest that for the acetyl group, in contrast to the ethoxycarbonyl group, more effective π-acceptor conformers like **9a** and **9b** are more populated than are conformers like that of structure **10**. A corollary of the increased effective π-acceptor character of the acetyl group is that the tautomeric equilibria for conformer species like **9a** and **9b** should be shifted to the right. Thus, the energy level diagram on the right side of Figure 8C (darkened arrows), for which $\Delta HOMO < \Delta LUMO$, becomes more pertinent. Since the occurrence of sign inversion (negative Q_0^x *B* terms) dictated by this diagram is not complete, it appears, however, that the populations of conformer species like **10**[77] and the horizontal tautomers (**11**) are still not negligible. These are schematically indicated by the energy level diagram (again, the

(78) (a) In dichloromethane, absorptions bands I and II (but not III and IV) commonly shift to higher energy at 199 K. A general blue shift in the absorption bands of metallo and free-base porphyrins on going to lower temperatures has been reported: (b) Edwards, L.; Dolphin, D. H.; Gouterman, M. *J. Mol. Spectrosc.* **1970**, *35*, 90.

Table IV. Monosubstituted Porphine HOMO and LUMO Energy Differences (eV) Calculated from INDO/S

substituent	ΔHOMO[a]	ΔLUMO[a]	ΔHOMO − ΔLUMO	exptl compd[b]	$10^{-4}B(Q_0^x)$[c]
methyl[d]	0.52	0.12	0.40	**1**	22.02
vinyl	0.54	0.13	0.41	**2**	21.61
cyano	0.47 (0.49)	0.23 (0.07)	0.24 (0.42)	**6, 7**	bisignate
methoxycarbonyl				**3**	2.76
60° rotated	0.47	0.20	0.27		
planar	0.44	0.32	0.12		
acetyl				**4, 5**	bisignate
60° rotated	0.48 (0.49)	0.19 (0.04)	0.29 (0.45)		
planar	0.44 (0.47)	0.32 (0.15)	0.12 (0.32)		
formyl	0.44	0.34	0.10	**8**	−7.53

[a] Values refer to the planar conformation of the vertical tautomer; horizontal tautomer values are in parentheses unless otherwise indicated. [b] Structures shown in Figure 1. [c] Values from Table I for band I; units are $D^2\ \beta_e/cm^{-1}$. [d] Calculated values are averages of both tautomers of methylporphine for the sake of comparison with OEP (1), which is symmetric with respect to tautomerism.

darkened arrows) on the left side of Figure 8C. There ΔHOMO > ΔLUMO and positive Q_0^x *B* term MCD is dictated. Thus, the observed bisignate MCD of band I for the acetyl porphyrins (Table I, Figure 3) can be seen to have a very reasonable explanation on the basis of structural effects alone. Consistent with this explanation is the fact (Table III) that the total *B* value of the MCD within band I of P-$COCH_3$ (**4**) changes from positive to negative on going from 295 to 199 K. The bisignate shape (see Figure 1, ref 1), however, is retained.

Finally, the broader range of spectrally distinguishable species present in solutions of P-$COCH_3$ should be evident in the absorption spectrum as well. The spectral deconvolution over absorption band I shown in Figure 13 clearly indicates this to be the case. At low temperature the dipole strength of band I decreases, the band blue shifts, and the shape of the band becomes more symmetrical.

(v) Formyl Group. In proceeding through the series of carbonyl-substituted porphyrins dual progression has been made in the decreasing effective steric bulk of the substituents and in the increasing π-acceptor character of the substituents. These attributes converge for the formyl group, and in the present series of porphyrins, having a methyl group adjacent to the chromophoric substituent, P-CHO (**8**) is the only porphyrin to exibit definitive sign inversion in the MCD associated with the Q_0^x transition *and with* the Q_0^y transition (Figure 4). This indicates that for most of the molecular species present ΔHOMO < ΔLUMO. In addition, since the Soret MCD of P-CHO is almost inverted, |ΔHOMO − ΔLUMO| is relatively large.

If the large open arrows in Figure 8C reflect the relative energies of the formyl porphyrin HOMO's and LUMO's, then sign inversion in the MCD of the visible Q_0^x and Q_0^y transitions would be expected for both tautomeric species **11** and **12**. Nevertheless, since the magnitudes of *B* terms relate roughly to the value of |ΔHOMO − ΔLUMO|, lower temperatures (which favor tautomer **12**) should result in larger negative and larger positive *B* values for the MCD associated with the Q_0^x and Q_0^y transitions, respectively. It is also unlikely that exact coplanarity obtains for formyl porphyrins having adjacent methyl groups, and, in fact, recent work by Chang et al.[56] indicates that the out-of-plane angle in the solid state is about 5%. In solution, the average angle may well be even larger owing to thermal motion. The anticipated increase in the magnitude of the MCD associated with band I due to either or both of these factors is indeed observed at 199 K (Table III) and is accompanied by a decrease in the dipole strength. The shape is also somewhat distorted owing to loss of intensity on the red edge of the band.

INDO/S Tracking of Orbital Energy Shifts due to the Conjunctive Interaction of Tautomerism and Substituent Group Stereochemistry. Preliminary to a more detailed and systematic theoretical study,[79] we have explicitly calculated the ground-state orbital energies of a series of model compounds using an all-valence-electron INDO/S method[80a-e] with two-center repulsion integrals evaluated by an empirical Mataga–Nishimoto–Weiss formula.[80f,g] The model compounds studied were derived from the monosubstituted porphyrins **2–8** shown in Figure 1 by replacing all perimeter alkyl groups with hydrogen atoms, except in **3**, where X = CO_2CH_3 rather than $CO_2C_2H_5$. The geometry of the porphyrin ring was taken from the symmetrized crystal geometry of protoporphyrin IX dimethyl ester.[71a] Standard bond lengths and angles were used for the substituent groups. Only trans tautomers were considered with the protons in plane at a N–H bond distance of 0.95 Å. The effect of nonplanarity between the porphyrin and substituent π systems was studied by rotating about the carbon–carbon single bond linking the substituent to the pyrrole ring.

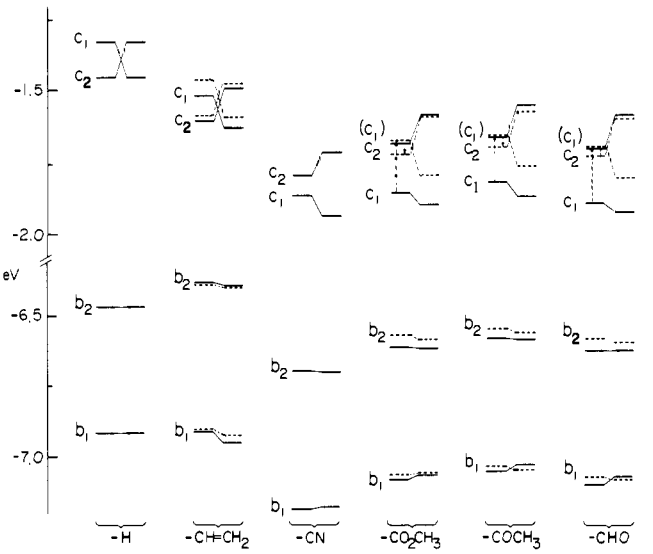

Figure 9. Effect of conformation and tautomerism on INDO/S HOMO and LUMO energies of free-base monosubstituted model porphines. Solid bars indicate planar conformers; broken bars indicate 60° out-of-plane conformers. Orbital labels from Figures 7E and 8C are retained. Energy levels for horizontal tautomers are on the left.

Figure 9 illustrates the calculated energies of the four frontier molecular orbitals for both "horizontal" (substituent ring is protonated) and "vertical" (substituent ring is not protonated) trans tautomers (shown in adjacent columns) of free-base and monosubstituted model porphyrins (solid lines) as well as for an arbitrary 60° out-of-plane conformation (dashed lines) for each of the substituents. The 60° rotation was chosen to dramatize the effect of loss of coplanarity.

(79) Goldbeck, R. A.; Waleh, A.; Loew, G. H., study in progress.

(80) (a) Zerner, M. C.; Ridley, J. E. *Theor. Chim. Acta* **1973**, *32*, 111. (b) Ridley, J. E.; Zerner, M. C. *Ibid.* **1976**, *42*, 223. (c) Bacon, A. D., Ph.D. Dissertation, University of Guelph, Guelph, Canada, 1976. (d) Bacon, A. D.; Zerner, M. C. *Theor. Chim. Acta* **1979**, *53*, 21. (e) Zerner, M. C.; Loew, G. H.; Kirchner, R. F.; Mueller-Westerhoff, U. T. *J. Am. Chem. Soc.* **1980**, *102*, 589. (f) Weiss, C., unpublished results. (g) Mataga, N.; Nishimoto, K. *Z. Phys. Chem. (Wiesbaden)* **1957**, *13*, 140.

A recent photoelectron spectrum of vapor-phase porphine[81] indicates first and second ionization potentials of 6.9 and 7.2 eV, which are in reasonable agreement with the calculated first and second HOMO energies of −6.5 and −6.9 eV. The calculated HOMO energy difference, ΔHOMO, of 0.4 eV is in particularly good agreement with the observed difference of 0.3 eV. The calculated HOMO energy difference is also consistent with values from previous ab initio,[82] Xα[83] and semiempirical PPP,[84] CNDO,[85] and INDO[75] calculations for free-base porphine which are generally between 0.1 and 0.5 eV.

The sensitivity of the orbitals in Figure 9 to energy lowering by an electron-withdrawing substituent shows the ordering $c_1 > c_2 > b_1 > b_2$. Thus, explicit calculations confirm the expectation (Figure 8C) that the largest and most important effect will be the shift in LUMO energies. The substituents are arranged in Figure 9 in order of increasing ΔLUMO (see also Table IV). This gives the same ranking for perturbative strength of the substituents as was arrived at earlier from the experimental spectral shift data and intuitive arguments. The large +I effect expected for cyano is also borne out by the calculations as evidenced by the general lowering of orbital energies for cyano in Figure 9.

Tautomerism is seen to have little effect on the HOMO energies but a large effect on LUMO energies. On going from the horizontal to vertical tautomer, c_2 is raised in energy while c_1 is simultaneously lowered a comparable amount. Substituent conformation also has a relatively small effect on HOMO energies, while the effect on LUMO energies can be large depending on the substituent. For the weakly perturbing vinyl group there is little effect, but twisting the strongly perturbing carbonyl groups out-of-plane tends to reverse the lowering of c_1 relative to c_2.

Michl's perimeter model[15a,b] predicts that, for not too strongly perturbing substituents, the dominant μ^+ contribution to MCD will yield an approximately linear proportionality between B values and the orbital energy difference ΔHOMO − ΔLUMO. A comparison of calculated orbital energy differences for the model compounds with the observed monosignate MCD of monosubstituted alkyl porphyrins is presented in Table IV. The calculated values of ΔHOMO − ΔLUMO decrease nearly monotonically with decreasing B value and thus show a reasonable correlation with Michl's perimeter model. However, the absolute magnitudes of ΔHOMO and ΔLUMO cannot directly account for MCD sign inversion since ΔHOMO − ΔLUMO is always calculated to be positive.

(i) Carbonyl Porphyrins. As noted in the preceding section, the close similarity in the pattern of HOMO and LUMO energies of the carbonyl porphyrins can be reconciled in terms of the Michl model with their qualitatively different Q_0^x MCD (monopositive, bisignate, and mononegative) by considering the effect of substituent conformation coupled with that of tautomerism. The decreasing steric bulk of the carbonyl groups suggests a shift from strongly out-of-plane conformers to nearly planar conformers proceeding from ethoxycarbonyl to formyl substitution, with acetyl presenting an intermediate case where both in- and out-of-plane conformers may be important.[77] Considering, for the moment, only the vertical tautomers in Figure 9 for the carbonyl porphyrins, the planar acetyl conformer is expected to give an inverted (negative B value) MCD similar to that actually observed for the formyl porphyrin (**8**) since both are calculated to have closely similar values of ΔHOMO − ΔLUMO (see also Table IV). Similarly, one expects from the orbital energy diagram and Table IV that a strongly out-of-plane conformer of an acetyl porphyrin (**4** and **5**) should show normal (positive B value) MCD, as is observed for the ethoxycarbonyl porphyrin (**3**). Attributing bisignate Q_0^x MCD in the acetyl porphyrins (**4** and **5**) to the presence of vertical and horizontal tautomers is not supported by Figure 9 for the twisted species since the energy levels calculated for them indicate that both tautomeric forms should give normal Q_0^x MCD, but the possibility of oppositely signed MCD is indicated for the two tautomers of planar carbonyl porphyrins.

(ii) Cyanoporphyrins. The bisignate MCD of the cyano porphyrins is difficult to rationalize on the basis of the calculated orbital energies and the Michl model. A tautomeric explanation of the bisignate MCD of the cyano porphyrins would attribute the inverted and normal MCD contributions to the presence of vertical and horizontal tautomers, but the calculated ΔHOMO − ΔLUMO values of 0.24 and 0.42 eV for the vertical and horizontal tautomers, respectively, both lie in the range (above 0.2 eV) expected from Table IV to correlate with positive B values. Thus, the present orbital energy calculations are inconsistent with the clearly bisignate MCD observed for one of the cyano porphyrins (**6**).

Background Vibronic MCD Effects. As noted in preceding sections, we have encountered one disturbing case, that of the cyano porphyrins P-CN (**6**) and MP-CN (**7**), where the MCD associated with their Q_0^x transitions (Figure 4) is significantly different although both exhibit essentially identical dual absorption bands. This occurs for an orbital energy distribution which leads to weak MCD for the Q_0^x and Q_0^y transitions and weak absorption for the Q_0^x transition and thus signals the need to specifically consider the extent to which vibronic effects may obscure the direct elucidation of structural effects since the dipole strengths of the Q_0^x transitions of the other carbonyl-substituted porphyrins are also quite small.

Hansen[86] has recently given a line-shape model for interference effects and Stephens[40c] has emphasized the moment analysis approach for treating the MCD associated with vibration-induced MCD. For porphyrins, specific investigations of vibronic MCD have largely centered on D_{4h} metallo porphyrins[23-25] although Perrin[87] has extended her earlier analysis[24] to D_{2h} porphyrins and has noted how the occurrence of both a_g and b_{1g} vibrations within the Q_1^x and Q_1^y manifolds leads to a different distribution[62] of MCD as compared to absorption intensity for these bands.

Here, we are not concerned with the MCD associated with the main Q_1^x and Q_1^y transition envelopes per se, but rather with low-frequency vibrational modes in and close to the Q_0^x envelope. In order to emphasize this concern, we have entered in Table I, in addition to the data for the multiple bands clearly evident in the spectra, two sets of numbers for the dipole strengths (unenclosed and enclosed in square brackets) and the MCD (enclosed in braces and in square brackets) associated with band I. Together, these data and the data obtained for cases where the components are evident provide a measure of underlying electronic bands due to different molecular species and a measure of how much MCD or absorption intensity may be due to low-frequency vibronic components. It can be noted in Table I that the differences between the FB fit (or the moment data for MCD) and the TLE fit data (see Experimental Section) for both absorption and MCD range from being minimal (P-$CO_2C_2H_5$) to significant (10 and 19% for the MCD and absorption spectra of OEP, respectively) to quite large (e.g., 44% for absorption band I of P-$COCH_3$). As an additional means of analysis, we also have included curve-fitting results for three pertinent cases—OEP, P-$COCH_3$, and P-CN in Figures 10–12, respectively.

(i) Octaethylporphyrin. The absorption maximum of band I of free-base porphyrins is commonly taken to roughly mark the electronic origin of the lowest energy transition. However, a number of studies of the quasi-line fluorescence and fluorescence excitation spectra of porphine and of octaalkylporphyrins in *n*-alkane matrices at 77 K indicate that the envelope of band I is comprised, in addition, of a number of low-frequency vibrational

(81) Dupuis, P.; Roberge, R.; Sandorfy, C. *Chem. Phys. Lett.* **1980**, *75*, 434.
(82) (a) Amlöf, J. *Int. J. Quantum Chem.* **1974**, *8*, 915. (b) Spangler, D.; Maggiora, G. M.; Shipman, L. L.; Christoffersen, R. E. *J. Am. Chem. Soc.* **1977**, *99*, 7470. (c) Sekino, H.; Kobayashi, H. *J. Chem. Phys.* **1981**, *75*, 3477.
(83) Sambe, H.; Felton, R. H. *Chem. Phys. Lett.* **1979**, *61*, 69.
(84) Sundbom, M. *Acta Chem. Scand.* **1968**, *22*, 1317.
(85) (a) Maggiora, G. M. *J. Am. Chem. Soc.* **1973**, *95*, 6555. (b) Yip, K. L.; Duke, C. B.; Salaneck, W. R.; Plummer, E. W.; Loubriel, G. *Chem. Phys. Lett.* **1977**, *49*, 530. (c) Chantrell, S. J.; McAuliffe, C. A.; Munn, R. W.; Pratt, A. C.; Weaver, R. F. *Bioinorg. Chem.* **1977**, *7*, 283.
(86) Hansen, A. E. In "Intramolecular Dynamics"; Jortner, J., Pullman, B., Eds.; D. Reidel: Boston, MA, 1982; pp 89–96.
(87) Perrin, M. H. *J. Chem. Phys.* **1973**, *59*, 2090.

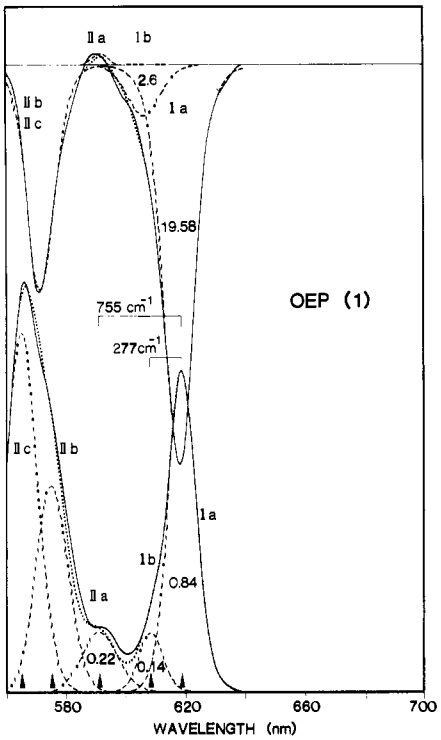

Figure 10. Approximate multiband fit for absorption and MCD bands I and II of OEP (1). The solid lines are the experimental spectra. The dotted lines indicate departures of the fitted spectra from the experimental spectra. The dashed lines are the component band shapes. The absorption curve was fitted using the program SPECDDP (Experimental Section). The absorption band parameters for bands Ia, Ib, and IIa served as initial input parameters for fitting the MCD spectrum using the program SPECFIT. MCD band II was fitted with a single shape function. The arabic numerals associated with each band are the dipole strengths and B values ($\times 10^{-4}$) obtained from the multiband curve-fitting protocol and thus differ from the values entered in Table I.

components of, in the D_{2h} point group, a_g and b_{1g} symmetry.[88] These results also obtain general support from resonance Raman studies.[89] Normal coordinate analysis[89b] suggests that the low-frequency modes (up to 800 cm^{-1} for porphine) are primarily associated with deformation vibrations of the methine bridges, and investigations of alkylated porphyrins[89b-d] show that these modes are quite sensitive to the presence of alkyl groups along the perimeter. More recently, Even and Jortner[90] have used laser-induced fluorescence excitation spectra to examine the electronic vibrational structure of porphine obtained as isolated ultracold molecules by the technique of supersonic expansion. These results support those obtained by the Shpol'skii method but avoid the site problems which plague the latter measurements.

In the ultracold spectrum of porphine, the strongest low-frequency vibronic modes are found at $\nu_0 + 148$, 304, and 712 cm^{-1}. In the Shpol'skii spectra[88] of OEP the strongest vibrational bands are found at roughly the same positions. In the very low resolution room-temperature solution absorption and MCD spectra of OEP shown in Figure 10, we do not observe a band corresponding to the 148-cm^{-1} mode, but the bands at $\nu_0 + 277$ cm^{-1} (band Ib) and

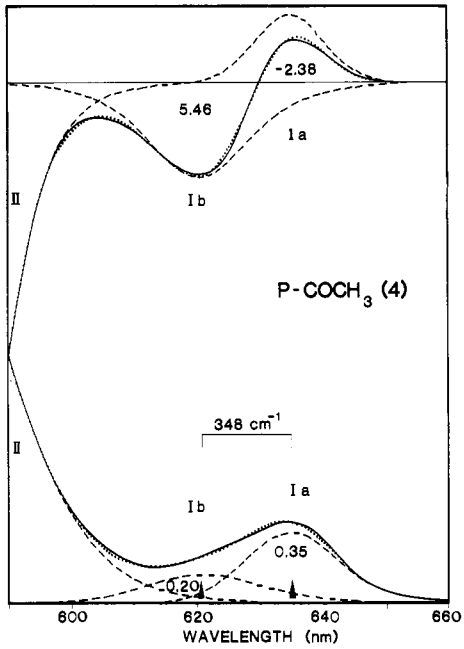

Figure 11. Two-band fit of the absorption and MCD of band I of P-C-OCH_3 (4) obtained with the program SPECABD (Experimental Section). Solid, dashed, and dotted lines have the significance denoted in the legend for Figure 10. B values are $\times 10^{-4}$.

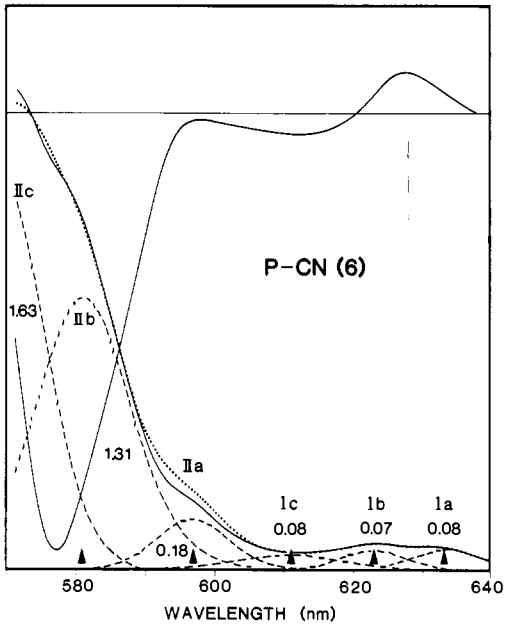

Figure 12. Multiband fit of the absorption associated with bands I and II of P-CN (6). The values for the dipole strengths differ from those entered in Table I owing to the inclusion here of band Ic. A satisfactory corresponding multiband fit could not be obtained for the MCD curve and is not shown. The vertical dashed line emphasizes the disparity between component features in the absorption and MCD spectra.

$\nu_0 + 755$ cm^{-1} (band IIa) do appear to correlate with the two higher frequency modes observed at high resolution. Of the two, only band Ib presents a possible hazard in the interpretation of the MCD associated with band I of the substituted porphyrins.

(ii) Acetyl Porphyrins. From what has just been pointed out for OEP, it might be reasonable to suppose that band Ib which has been fitted beneath absorption band I of P-$COCH_3$ (Figure 11) is entirely of vibrational origin and thus that the negative MCD band (Ib) is of like origin whereas our structure based interpretation (vide supra) attributed band Ib primarily to conformers like structure **10** and band Ia to conformers like **9a** and **9b**, each consisting of an electronic origin and associated (but unresolved) low-frequency vibrational components.

(88) (a) Gradyushko, A. T.; Solov'ev, K. N.; Starukhin, A. S. *Opt. Spectrosc.* **1976**, *40*, 267. (b) Bykovskaya, L. A.; Gradyushko, A. T.; Personov, R. I.; Romanovskii, Y. V.; Solov'ev, K. N.; Starukhin, A. S.; Shul'ga, A. M. *Zh. Prikl. Spektrosk.* **1978**, *29*, 1088. (c) Arabei, S. M.; Shkirman, S. F.; Solov'ev, K. N.; Yegorova, G. D. *Spectrosc. Lett.* **1977**, *10*, 677. (d) Solov'ev, K. N.; Shkirman, S. F.; Zagusta, G. A. *Zh. Prikl. Spektrosk.* **1971**, *14*, 1055.

(89) (a) Plus, R.; Lutz, M. *Spectrosc. Lett.* **1974**, *7*, 133. (b) Solov'ev, K. N.; Gladkov, L. L.; Gradyushko, A. T.; Ksenofontova, N. M.; Shul'ga, A. M.; Starukhin, A. S. *J. Mol. Struct.* **1978**, *45*, 267. (c) Gladkov, L. L.; Gradyushko, A. T.; Ksenofontova, N. M.; Solov'ev, K. N.; Starukhin, A. S.; Shul'ga, A. M. *Zh. Prikl. Spektrosk.* **1976**, *27*, 1188. (d) Gladkov, L. L.; Gradyushko, A. T.; Solov'ev, K. N.; Starukhin, A. S.; Shul'ga, A. M. *Ibid.* **1978**, *29*, 304.

(90) Even, U.; Jortner, J. *J. Chem. Phys.* **1982**, *77*, 4391.

While we recognize that a vibronic background must generally be present, we believe that a structural explanation is valid in large part for several reasons: (i) the MCD spectrum of P-$COCH_3$ can be viewed as analogous to the sum of the spectra of the sterically constrained P-$CO_2C_2H_5$ and that of the more rotationally mobile P-CHO; (ii) at low temperature (Table III; Figure 1, ref 1) MCD band Ib becomes smaller while MCD band Ia becomes larger—just the result expected for both conformational and tautomer equilibria; (iii) the overall shape of MCD band I is not sensitive to structure (compare the spectra of P-$COCH_3$ and DP-2-$COCH_3$ in Figure 1 of ref 1 and the data in Table I) as would be expected (and is observed for the cyano porphyrins) if the low-frequency ring deformation modes were dominant in determining the shape; and (iv) the bisignate shape of band I for P-$COCH_3$ is not markedly sensitive to the particular solvent media as might be expected if ring-deformation modes played an important role.

The band shapes of both the MCD and absorption associated with the Q_0^x transitions of P-$CO_2C_2H_5$ (Figure 3) and P-CHO (Figure 4) are relatively symmetric; consequently, curve-fitting spectral analysis is of little value in assessing the importance of vibronic effects for them. Such effects are undoubtedly present but do not obscure structural conclusions (vide supra) based merely on the signs of their MCD bands.

(iii) Cyano Porphyrins. Although support for the structural effect of tautomerism can be surmised from the effect of temperature (Table III), background vibronic effects evidently do intrude at a higher level in the MCD and absorption associated with band I of the cyano porphyrins P-CN (**6**) and MP-CN (**7**) (Figure 4).

One aspect of the problem is illustrated in the expanded and partially curve-fit spectra shown for P-CN in Figure 12. In the structure biased interpretation of these spectra (vide supra), we suggested that the negative and positive MCD bands might arise from the horizontal and vertical tautomers (**11** and **12**, respectively) of P-CN and that absorption bands Ia and Ib corresponded to them. The spectra in Figure 12 show the disparity of this assignment. Further, while an absorption counterpart of the negative MCD band can be fitted in the absorption spectrum (band Ic), the MCD spectrum does not contain obvious counterparts to absorption bands Ia and Ib. The band splitting which is evident in the absorption spectrum could not be detected in the MCD spectrum at narrow slit settings, nor could two band shapes be made to account for the MCD intensity of the positive MCD band by curve-fitting. This is in marked contrast to the situations for OEP (Figure 10) and P-$COCH_3$ (Figure 11) wherein absorption and MCD intensity could be accounted for by an equal number of band shapes. Thus specific transition assignments are uncertain although the possibilities that (i) bands Ia and Ib are the electronic origins for tautomeric species, (ii) band Ia is an electronic origin and bands Ib and Ic are low frequency vibrational components, and (iii) band Ia is a hot band with little MCD intensity, might be retained.

Finally, other indications of the importance of low-frequency ring-deformation vibrational modes for the cyano porphyrins, in contrast to the acetyl porphyrins, are that the relatively minor structural differences between P-CN (**6**) and MP-CN (**7**) result in such markedly different MCD for band I and that the observed MCD band shapes for the cyano porphyrins are much more sensitive to the solvent medium (carbon tetrachloride, toluene, and chloroform) than are those of the acetyl porphyrins.

Conclusion

In this study of alkyl free-base porphyrins containing vinyl, cyano, ethoxycarbonyl, acetyl, and formyl groups as the single chromophoric substituents, we have presented the first optical evidence for structure effects which arise from the existence of substituent group conformational equilibria and from the existence of N–H proton equilibria. These effects are singularly evident in an MCD spectrum because of the signed nature of the phenomenon and because the different molecular species present in solution may exhibit oppositely signed MCD bands.

Some inference of the modulating effects of N–H proton tautomerism on the optical properties of substituted free-base porphyrins is garnered from the effects of temperature on the MCD of two cyano porphyrins. The vinyl group is a weakly perturbing substituent and few specific structural effect inferences can be drawn for it. Populations of well out-of-plane conformers appear to be important for porphyrins containing nuclear ester functions. A broader effective range of conformers contribute to the optical spectra of acetyl porphyrins. In the bisignate MCD observed for the Q_0^x transitions of two acetyl porphyrins, those for which the acetyl group is well out of plane are thought to give rise to the negatively signed MCD lobe whereas those for which π orbital overlap is more optimal give rise to the positive lobe. For the formyl group, more nearly coplanar conformations are highly populated. In addition, we have considered the possibility that vibronic effects may intrude at the same level as structural effects and thereby obscure a structure-based interpretation of the spectra. This does not appear to be the case except for the cyano porphyrins.

Additional information about substituent effects can be derived from porphyrins specifically constructed to embody more or fewer steric interactions. Work along these lines is in progress.[42,79]

As a final comment, we feel that the present work underscores recent concern with the way substituent group geometry may modulate the biological activities of some heme proteins during their reaction cycles.

Acknowledgment. We are indebted to Mrs. Ruth Records for her diligence and perseverance in obtaining the spectra. We are also particularly indebted to our former colleagues Drs. Robert E. Linder and Günter Barth for the flexible curve-fitting and moment analysis programs they have devised. Financial support for this work was generously provided in part by grants from the National Science Foundation (CHE 80-25733 to C.D. and PCM 79-21591 to A.W. and G.H.L.), the National Institutes of Health (GM-20276), and the Australian Research Grants Committee.

Registry No. 1, 2683-82-1; **1a**, 865-16-7; **2**, 42749-20-2; **3**, 63900-88-9; **4**, 63940-11-4; **5**, 13003-76-4; **6**, 90508-48-8; **7**, 90508-49-9; **8**, 62786-91-8.